UNIVERSITY OF CENTRAL OKLAHOMA
SCHOOL OF ENGINEERING

CELL-DRIVEN COLLAGEN MATRIX REMODELING MEASURED WITH OCT

by

Joshua Pitzer

Prepared under the direction of Dr. Gang Xu

Thesis presented to the Jackson College of Graduate Studies of
The University of Central Oklahoma in partial fulfilment of the
Requirements of the degree of
MASTER OF SCIENCE
April 2026
Edmond, Oklahoma

UNIVERSITY OF CENTRAL OKLAHOMA
SCHOOL OF ENGINEERING

ABSTRACT

CELL-DRIVEN COLLAGEN MATRIX REMODELING MEASURED WITH OCT

BY: Joshua Pitzer
ADVISOR: Dr. Gang Xu

April 2026
Edmond, Oklahoma

Fibroblast-driven compaction and tension generation in the collagen matrix leads to changes of the mechanical microenvironment that are important for the regulation of these cells' differentiations and functions. Yet routine, region-specific measurements of elastic modulus of developing fibroblast-populated collagen matrices (FPCM) remain challenging. This work refined and validated an optical coherence tomography (OCT) based microindentation assay that uses a spherical glass bead as the indenter. The applied load is simply the bead's weight minus buoyancy, so indentation force is known without complex calibration. OCT provides an accurate, detailed surface indentation profile of the developing FPCM in real time. Using the Hertz contact formula for the spherical-indentation model converts these OCT measurements into local elastic modulus of FPCM during cell-dependent compaction and tension generation. The method was verified through testing against reference silicone gels with known elastic moduli. This project also assessed practical operating ranges by varying bead weight to achieve relatively small indentation depths on soft matrices. Applied to FPCM, the assay revealed progressive stiffening (increased elastic modulus) together with thinning and volume loss while the attachment area remains largely constant, consistent with cell-driven compaction and remodeling. In summary, the OCT-based approach provides a minimally invasive, spatially resolved tool for quantifying elasticity of collagen matrices and related biomaterials, supporting studies of wound healing, fibrosis modeling, and tissue-engineering applications.

Contents

Acknowledgements

I would like to express my sincere gratitude to Dr. Gang Xu for his guidance and mentorship throughout this thesis process. His support was instrumental in shaping this work from its early stages through completion. The opportunity to attend the Biophysical Society Conference in San Francisco, which he facilitated, was particularly impactful in advancing this research and broadening my understanding of the field. This project was iterative, and his step-by-step guidance was essential in refining both the methodology and interpretation of results.

I would also like to thank my thesis committee members, Dr. Mohammad Hossan and Dr. Melville Vaughan, for their time, support, and willingness to serve on my committee. Their participation and feedback contributed meaningfully to the development of this work.

I am grateful to my father, Kurt Pitzer, whose encouragement to pursue a master's degree set this entire journey in motion. Without his initial push, this path—including the completion of this research—would not have begun.

I would like to thank my brother, Joseph Pitzer, for his continued guidance and support throughout my academic career. Having completed engineering before me, he provided both practical advice and academic perspective that helped me navigate the challenges of this program.

Finally, thank you to my haters. There were plenty of people who told me I don't have to get a master's degree. They told me that no one requires me to have a master's degree and that I am delaying my career. Those perspectives ultimately reinforced my decision to invest time in work that I found meaningful. I am making a point to spend more time doing things I want to do rather than doing things I have to do.

1 Introduction

1.1 Background

Collagen supports the mechanics of cells as it is the primary structural protein in the extracellular matrix (ECM) of connective tissues [1]. In the natural repair process, the common type I collagen reacts during wound healing [2]. ECM producing cells, fibroblasts, synthesize the collagen and actively remodel the matrix to preserve tissue integrity [3]. As part of the active wound healing process, fibroblasts will differentiate into contractile myofibroblasts. The myofibroblasts will contract collagen which draws together the wound edges [3]. This cell driven remodeling increases the stiffness and strength of the healing tissue over time [4]. However, excessive fibroblast activity can cause problems or scarring known as fibrosis [3]. In wound healing research, it is necessary to understand how cells mechanically interact with and remodel collagen matrixes. This understanding extends to other areas as well, including designing better therapies to control fibrosis and for tissue engineering [3].

Researchers can study collagen remodeling in a controlled environment. In doing so, they will often use three-dimensional collagen matrices as in vitro models. Under normal pH conditions, collagen type I naturally forms a wet, fibrous gel. This gel behaves more like real tissue than the flat, stiff plastic surfaces usually used to grow cells [2]. Cells cultured in this 3-D collagen gel experience a soft flexible fibrous environment, which is vastly different from the rigid plastic substrate from a normal cell culture [3]. For instance, collagen gels can be as soft as 50 Pa, whereas plastic dishes can be as stiff as 1 GP [2]. The great difference and stiffness leads to a huge difference in the cell behavior, structure, and morphology with fibroblasts in soft collagen being branched and spread out compared to the flattened anchored fibroblasts on stiff substrates [3]. The 3D collagen matrix allows for limited adhesion points and a deformable scaffold, so therefore the cells engage different attachment proteins (integrins) and rearrange their cytoskeleton to move and apply force [3]. These different environments create unique, bio, mechanical cues which give feedback to regulate cellular functions like differentiation, movement, and growth [4]. When the collagen matrix becomes stiffer, cells sense this change through integrins and signaling pathways involving molecules like TGF-β1. This can cause fibroblasts to reinforce their cytoskeleton and even turn into myofibroblasts, which increase

contraction strength [5]. Cells on stiffer collagen also produce more mechanosensitive proteins such as $\alpha_v\beta_3$ integrins, showing that they become more active and tighter [5]. Hence, the relationship between the cells and the collagen matrix determine how cells develop and how the matrix ends up being shaped. Understanding these qualities is a vital aspect of tissue physiology.

1.2 Collagen Matrix Mechanics

Fibroblast within a collagen matrix will actively pull and move collagen fibers which leads to visible shrinking of the matrix and changes in mechanical properties [3]. This structure is known as a fibroblast populated cellular matrix (FPCM) [1]. Pulling through their Acton-myosin cytoskeleton, fibroblasts contract the collagen matrix and align the fibers in the direction of tension [3]. Every part of the matrix will shrink if it is not anchored. On the other hand, if the matrix were anchored to a stiff substrate, it cannot decrease much in circumference. The cells will pull harder, increase internal tension, and end up looking more like myofibroblasts with prominent stress fibers [3]. Such internal tension increases the stiffness, thereby increasing the modulus of elasticity. The anchored matrix stiffens for multiple reasons, including: fibers being packed closer together, fibers stretching, and aligning, and biochemical cross linking of collagen fibers [4]. Responding to the higher stiffness, cells will morph to a new mechanical equilibrium called tensional homeostasis [3]. Studies show that this compaction is entirely cell-driven, as the collagen itself does not compact [1]. Overall, Collagen matrix remodeling is a dynamic feedback loop in which cell forces remodel the matrix and change its stiffness. Those mechanical changes then influence how the cells continue to exert forces.

This feedback relationship between cells and the collagen matrix is foundational for natural healing, such as wound contraction and scar formation, and it is intentionally used in tissue engineering. Engineered tissues often start as populated collagen or ECM hydrogels that mature over time. The cells present create more matrix and pull on the scaffold, causing it to compact and gradually increase mechanical strength [4]. It's necessary to monitor the changes because the mechanical properties of a tissue construction are directly linked to its function [4]. For example, an engineered collagen based ligament or skin substitute has to have the right stiffness and tensile stress for it to function like the real tissue. Biomechanical cues will affect cell signaling,

such as matrix rigidity enhancing growth factor, signaling, or inducing differentiation of specific cells [3]. And so this ability of quantifying the evolution of matrix mechanics is very useful for biology and quality control in regenerative medicine [4].

1.3 Measuring Mechanical Remodeling of Collagen Matrices

Quantifying the mechanical changes in a collagen matrix as it remodels is not so simple. One qualitative approach is the collagen gel contraction assay, where one measures the shrinking over time of a cell populated collagen gel as a way of showing cell-generated force [7]. Even though shrinkage shows that cells are pulling, Matrix size alone does not directly provide material properties like stiffness or elastic modulus. Classical lab tests like shear rheometry or uniaxial tensile testing can measure the gel's stiffness and give you its overall elastic modulus. Rheology is a common method for measuring the mechanical behavior of soft gels by applying controlled shear deformation and recording the material's resistance; it usually reports a bulk-averaged property of the whole sample [18]. However, such tests often require invasive handling of the fragile gel and only provide a single bulk value for the whole sample rather than local region. In contrast, indentation based mechanical testing offers a nondestructive way to probe local stiffness in soft materials like collagen gels [4]. In a typical micro-indentation experiment, a rigid indenter, such as a solid sphere, is pressed into the matrix's surface and the resulting force is recorded as a displacement curve [4]. The Hertz contact model is a useful equation commonly applied to these data to uncover elastic properties [4]. Hertz's theory of elastic contact shows the relationship between the indentation force (F) and indentation depth (δ) for a sphere pressing on an elastic substrate, This reveals the material's Young's modulus but assumes an isotropic, linear elastic material [4]. Largely used in bioengineering, this equation is key in atomic force microscopy (AFM) indentation of cells and hydrogels, to estimate local Young's modulus [4]. Indentation testing is advantageous for being minimally invasive, repeatable on the same sample, and capable of mapping stiffness at different positions. It detects the small mechanical changes in soft biomaterials without destroying them. For these reasons, depth sensing micro-indentation has become a pivotal tool for charting mechanical properties in soft biomaterials [4].

Modern technology has brought together indentation and imaging to improve how we measure the mechanics of soft tissues. One of these methods is optical coherence elastography, which uses optical coherence tomography (OCT) to image tissue deformation under load. Then measurements can be obtained to calculate mechanical properties. OCT is a type of imaging that uses light interference to capture high resolution cross-sectional images of biological tissues or hydrogels in real time [4]. Since OCT can penetrate a few millimeters into tissue and provide micrometer-scale resolution, it is great for visualizing the interior deformation of a 3D collagen matrix without cutting it open [4]. These advantages can be leveraged with indentation to create OCT-based indentation systems in which a known force is applied through a spherical indenter. Then the OCT imaging beam scans the material to capture the resulting deformation profile [4]. From the OCT scans, one can directly measure the indenter depth and the material's deformation, and then apply Hertz's model (or other mechanical models) to calculate mechanical properties [4].

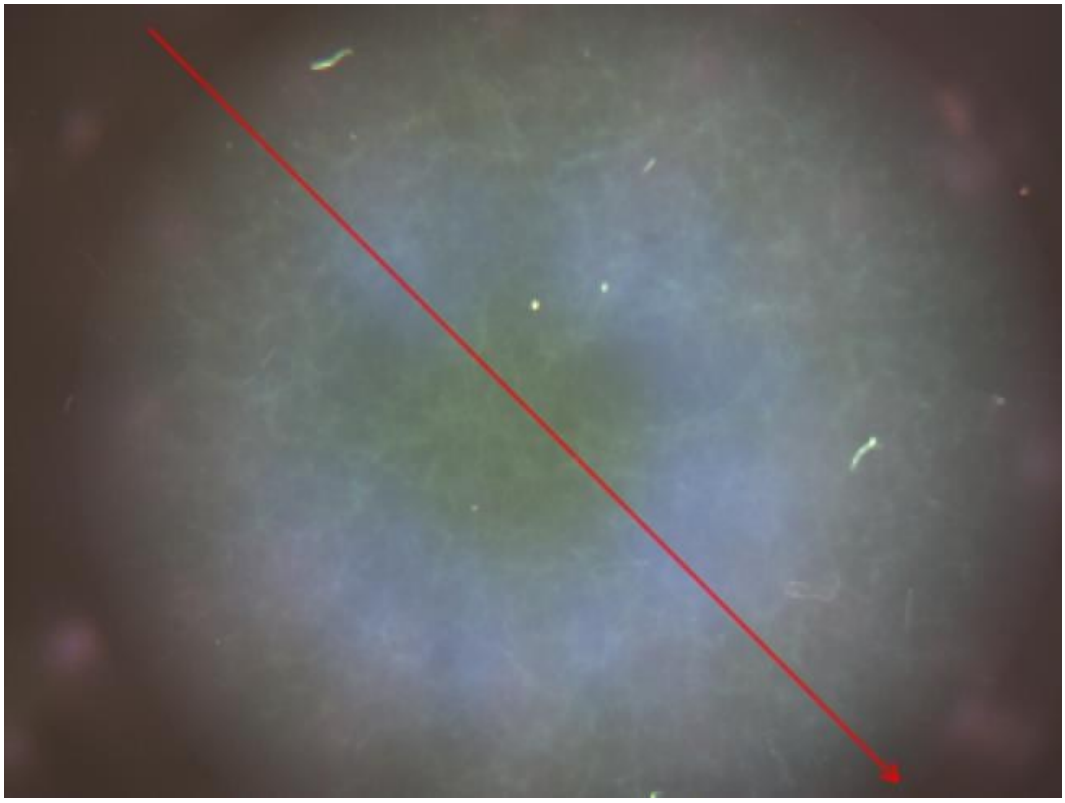

Figure 1.1: What the sample looks like in the OCT software before scanning. The round area is the fibroblast-populated collagen gel. The red line shows the exact path where the OCT beam scans across the sample. This scan produces a slice-like image of the matrix.

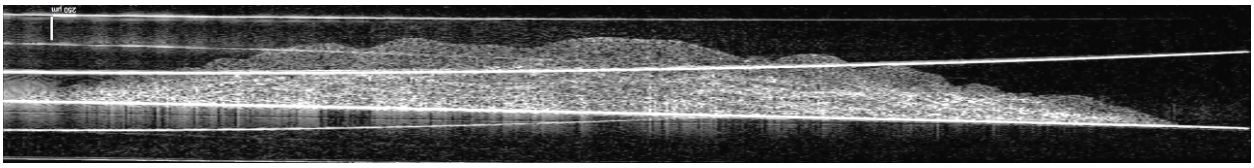

Figure 1.2: OCT cross-sectional image of a fibroblast populated collagen matrix (FPCM). This is a side-view "slice" through the collagen gel captured by the OCT system. This image helps visualize the shape of the matrix and is used to measure structural changes over time.

The combination of OCT with mechanical testing offers several important advantages for studying cell-driven matrix remodeling. First, It is minimally invasive as the small indenter gently "presses" the matrix without requiring grips. It provides a direct readout of a local mechanical response [4]. Second, the measurement can be made at a specified region (e.g. the center of an anchored gel) and repeated over time to monitor changes. Compared to AFM microindentation, this approach uses a larger indenter (0.5-1.5 mm in diameter) and a gravity-driven load, which produces deformations on a larger scale. This helps avoid extremely high local strains that sharp tips would induce [8]. By continuously tracking the mechanical properties, we gain insight into the dynamics of matrix remodeling. These properties can show how quickly and by how much a fibroblast-populated collagen gel stiffens over time, and how that correlates with cellular events like differentiation or alignment.

1.4 Scope of This Work

Given the need for an easy to use assay for quantifying collagen matrix remodeling, the focus of this thesis is on the development and validation of an OCT based method to measure cell driven collagen matrix mechanical changes. We present a system that uses OCT imaging with a small rigid bead to noninvasively measure the stiffness of collagen matrices being actively remodeled by cells. The bead acts as a spherical indenter, and its weight provides a known, calibrated force (equal to the bead's mass times gravity, minus buoyant force in the culture medium). This eliminates the need for complex force sensors or actuators. The force is known a priori from physical properties of the indenter. Then, we use optical coherence tomography to image the bead and the matrix in a cross section [1]. From the OCT captured cross section, we measure the

indentation depth of the matrix caused by the bead's weight. Given the indentation depth δ and the indenter radius R, we can calculate the local Young's modulus E of the matrix by applying the classic Hertz contact model for a spherical indenter [13].

We also explore the practical operating range of the assay. By varying the indenter material and size (steel vs. glass beads, diameters ~0.5-1.5 mm), we alter the applied load. A heavier bead provides a larger force, which is useful for stiffer samples that would otherwise yield too shallow an indentation to measure accurately. Conversely, a lighter bead improves sensitivity on ultra soft matrices where even a small load might produce large deformations. We report on the effect of bead weight on measurable indentation and discuss how to optimize the assay for very soft substrates. Overall, our goal is to demonstrate that this approach can reproducibly quantify local modulus of elasticity in soft materials, even if absolute values may differ from standard tests.

Ultimately, this method enables us to monitor how biomechanical cues and cellular forces work in real time. The ability to observe and quantify these processes non-invasively will advance our understanding of cell ECM mechanobiology, and could also inform the design of improved tissue engineering strategies and therapies for wound healing and fibrosis [4].

2 Materials and Methods

2.1 Cell Culture and Fibroblast Populated Collagen Matrix Preparation

Fibroblast populated collagen matrices were prepared under sterile cell culture conditions using methods adapted from previously published collagen lattice protocols [1], [6]. Fibroblasts were maintained in complete culture medium before matrix preparation. Vaughan et al. cultured fibroblasts in DMEM/high glucose supplemented with 5% fetal bovine serum and 1% antibiotic/antimycotic at 37°C and 5% CO_2 [1]. This published method guided the culture conditions used in this study.

Cells were detached, counted, and mixed into a cold type I collagen solution to prevent premature gelation. The collagen-cell mixture was prepared at approximately 0.65 mg/mL type I collagen and 125,000 cells/mL, following the anchored matrix protocol [1]. The mixture was gently pipetted to distribute cells evenly while avoiding bubbles.

To obtain a relatively wide, flat gel suitable for indentation, we employed a two-step dispensing method: first, ~230 µL of collagen-cell suspension was placed in the center of a culture dish; then ~90 µL was sucked back up after partial gelation as depicted in figure 2.1. This left an approximately 140 µL dome-shaped collagen gel, but critically, it spread to the diameter of a 230 µL drop. By creating a larger diameter (while using less volume), the matrix was thinner and broader making it easier to place the bead and to image the indentation without edge effects [1], [6].

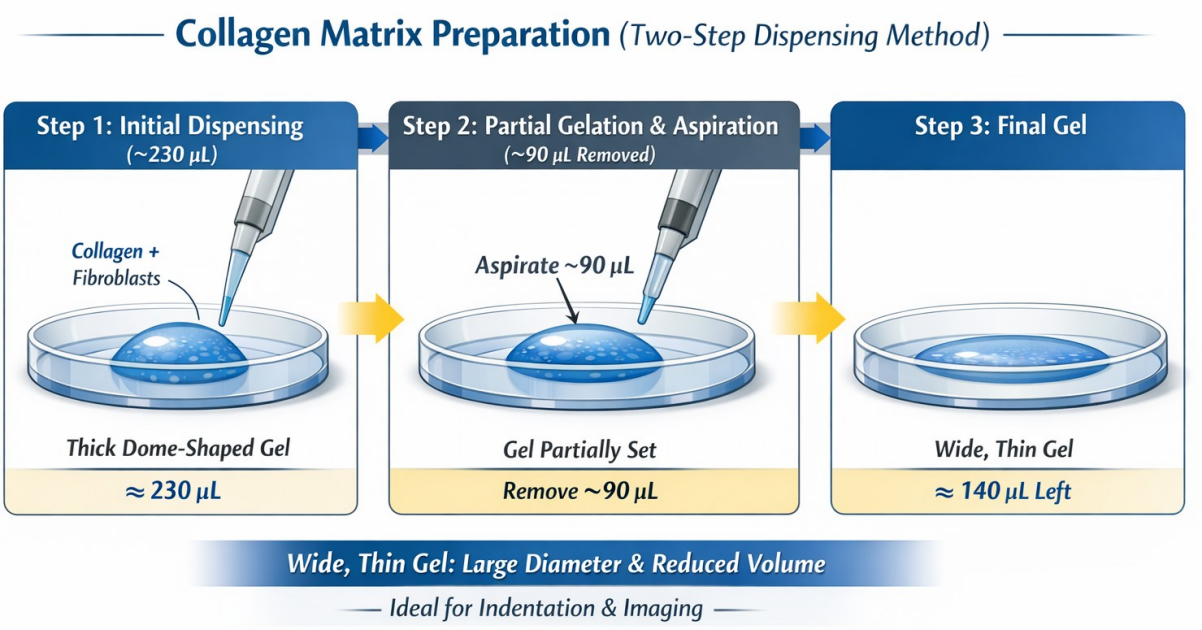

Figure 2.3: Wide matrix preparation (ChatGPT Generated)

After gelation, culture medium was added to each dish, and the matrices were incubated at 37°C and 5% CO_2. Six fibroblast populated collagen matrices were prepared. Four were maintained in standard culture medium as controls, and two were cultured with glyoxal added to the medium. Glyoxal can induce the formation of additional cross-links in collagen, which in many contexts is expected to increase stiffness and reduce gel contraction over time [8]. All matrices were kept in an incubator between measurements, and their medium (with or without glyoxal) was refreshed as needed over a 7-day period [1], [6].

2.2 OCT-Based Microindentation

We implemented a micro indentation experimental setup using small beads as indenters and OCT for deformation imaging. This approach allows us to directly observe how much a soft gel or tissue sample deforms under a known load, and then relate that deformation to the material's stiffness via the Hertz contact model [13]. The OCT system was arranged in an inverted configuration (with the imaging camera/lens facing upward). This inversion meant we could place our sample (e.g. a gel in a Petri dish or multi-well plate) above the OCT camera and drop the bead onto the sample from above without the imaging hardware obstructing the process. The

OCT captures cross-sectional images (B-scans) through the gel and bead. From the OCT cross-sections, we determined the indentation depth δ as the distance the bead had sunk into the sample. It is the vertical difference between the undeformed surface and the lowest point of bead surface contact.

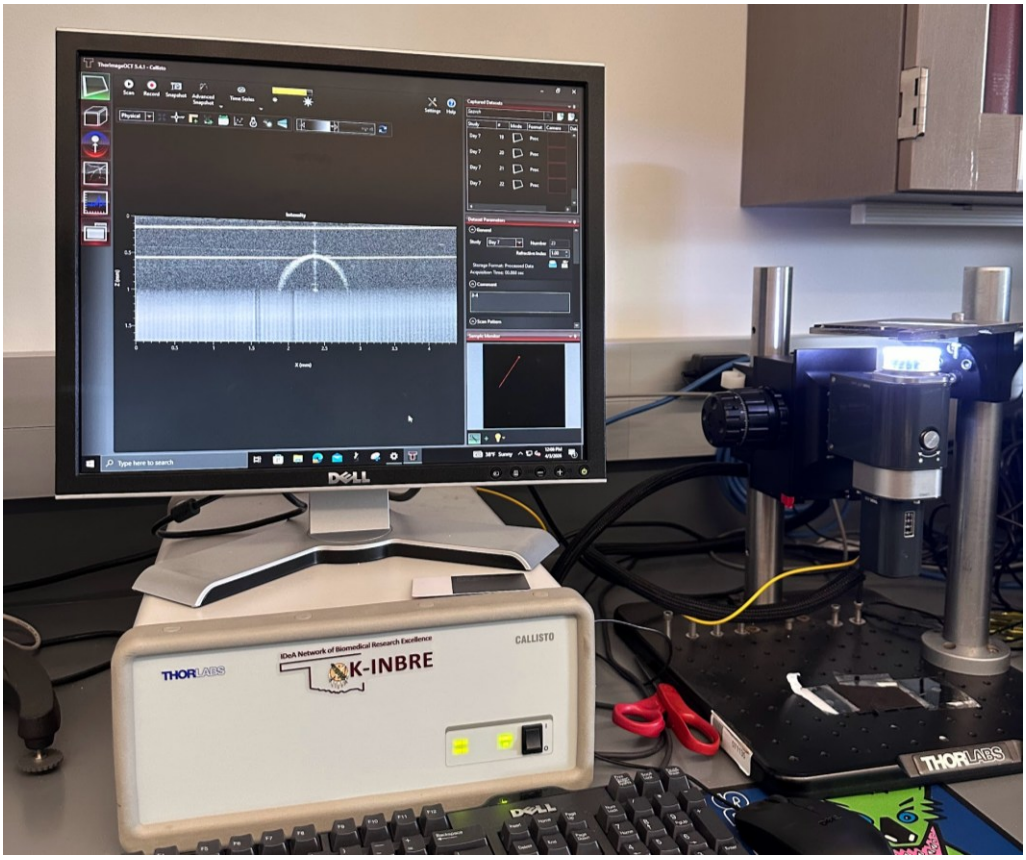

Figure 2.1: Inverted OCT setup and software interface

These tests were on wet samples, where the sample was submerged in culture medium or PBS, so buoyancy reduced the effective force. The indentation force F was thus calculated as:

$$F=F_b-F_f$$

$$F_b=V_{bead}\cdot\rho_{bead}\cdot g$$

$$F_f=V_{bead}\cdot\rho_{fluid}\cdot g$$

$$F=F_b-F_f$$

where m_{bead} and V_{bead} are the bead mass and volume (computed from its diameter and density), and ρ_{fluid} = 1.0 $\frac{g}{cm}^3$ is the fluid density. For a 0.5 mm glass bead, for example, mg = 1.60 μN and the buoyant force is ~0.64 μN, giving a net load F = 0.96 μN. For a 0.8 mm steel bead, F in medium was about an order of magnitude larger (~18 μN net). These forces were treated as constant (static load) during the indentation. No external microforce transducer was needed. Gravity provided a reproducible load, and its magnitude was determined by simple gravimetric calculation.

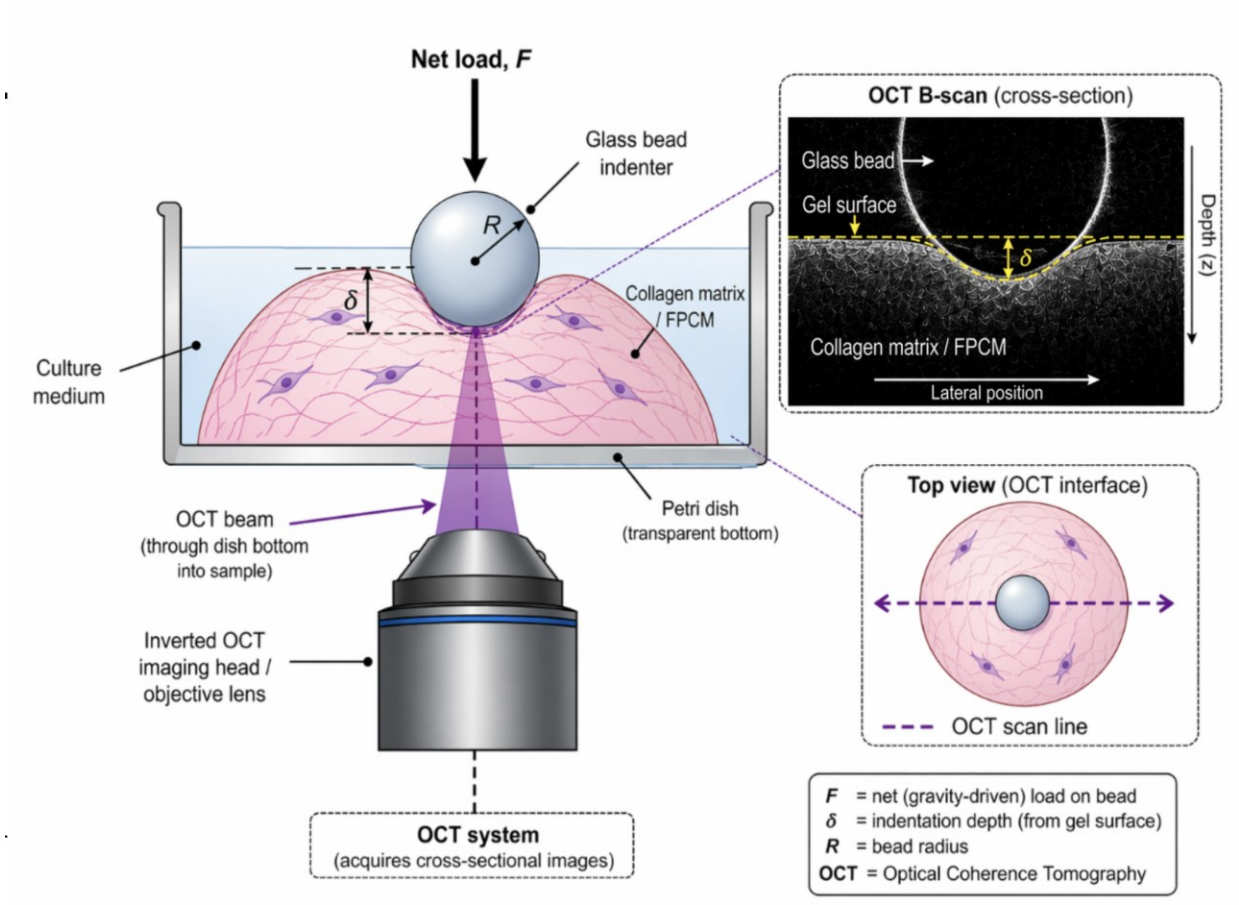

Figure 2.2: Diagram of OCT setup and bead indentation (ChatGPT Generated).

2.3 Hertz Model and Elastic Modulus Calculation

The Young's modulus E was calculated from the applied force F, spherical indenter radius R, and measured indentation depth δ using the Hertz contact model for a spherical indenter [13]. Assuming the sample behaves as a linear elastic material the Hertz equation reduces as follows:

$$F = \frac{4}{3}\frac{E}{1-\nu^2}\sqrt{R}\,\delta^{3/2}$$

assuming ν=0.5 for an incompressible matrix, the equation becomes

$$F = \frac{16}{9}E\sqrt{R}\,\delta^{3/2}$$

Solving for Young's modulus gives

$$E = \frac{9F}{16\sqrt{R}\delta^{3/2}}$$

where F is the applied force, R is the bead radius, and δ is the indentation depth [13].

This formula was implemented in a spreadsheet to compute E (in Pascals) for each indent test. We used measured values of F (in Newtons) and δ (in meters), and we converted R from mm to meters in the calculation. For example, for a nominally 2 kPa silicone gel tested with the 0.8 mm steel bead, we recorded an indentation depth δ=0.09 mm with R=0.4mm and F=18x10^-6 N. Plugging these into the Hertz equation yields E≈0.59 kPa. We applied this procedure to all samples, typically taking the average δ from two or more repeat OCT scans for robustness. For FPCM samples, multiple indentations (on separate, equivalently prepared lattices) were performed and averaged to account for sample variability.

2.4 Bead Indentation Experiments with OCT Imaging

Starting 24 hours after gelation (Day 1) and on each subsequent day up to Day 7, we performed a gentle indentation test on each collagen matrix using a 0.5 mm diameter glass bead as the

indenter. We chose a glass bead for the living matrices because glass has a much lower density (~2.5 g/cm³) than steel, resulting in a smaller weight force. This minimized the risk of over compressing or damaging the delicate cell-seeded gels. For each measurement, the Petri dish containing the matrix was placed on the inverted OCT stage, and the glass bead was carefully lowered onto the center of the gel's surface. The OCT system captured a cross-sectional image of the bead indenting the gel, from which we extracted the indentation depth. Assuming the force on the gel was the bead's weight minus buoyant force, we could then estimate the matrix's effective stiffness via the Hertz contact formula. Because the measurements were non-destructive, the same samples were measured repeatedly each day.

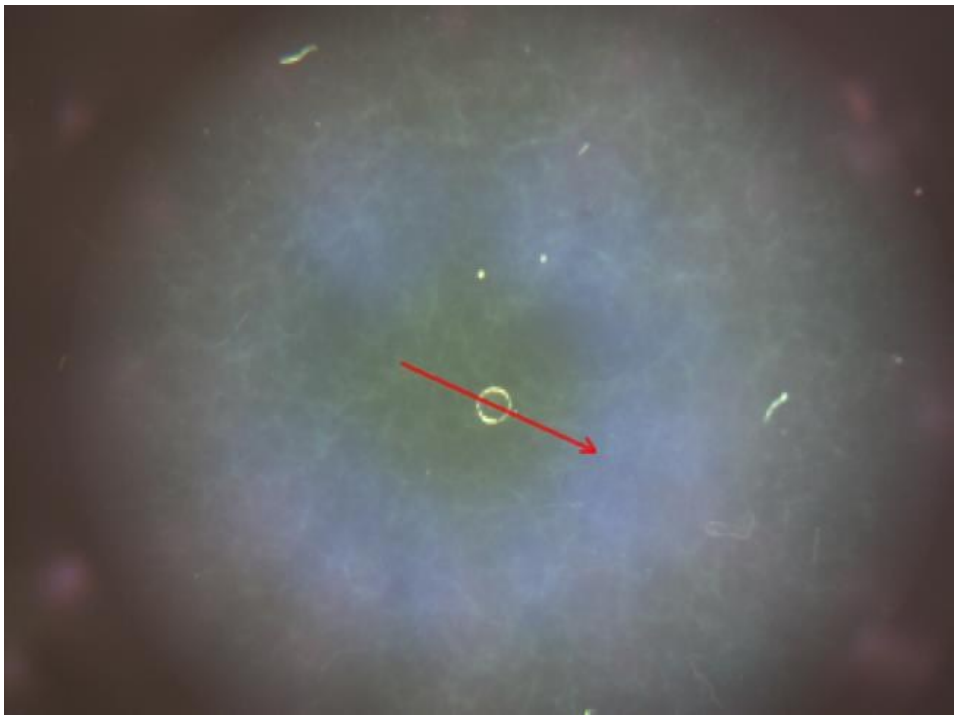

Figure 2.4: OCT camera view showing where the glass bead was placed on the collagen gel. The small bright circle near the middle is the glass bead used as the indenter. The red arrow is the OCT beam scan path.

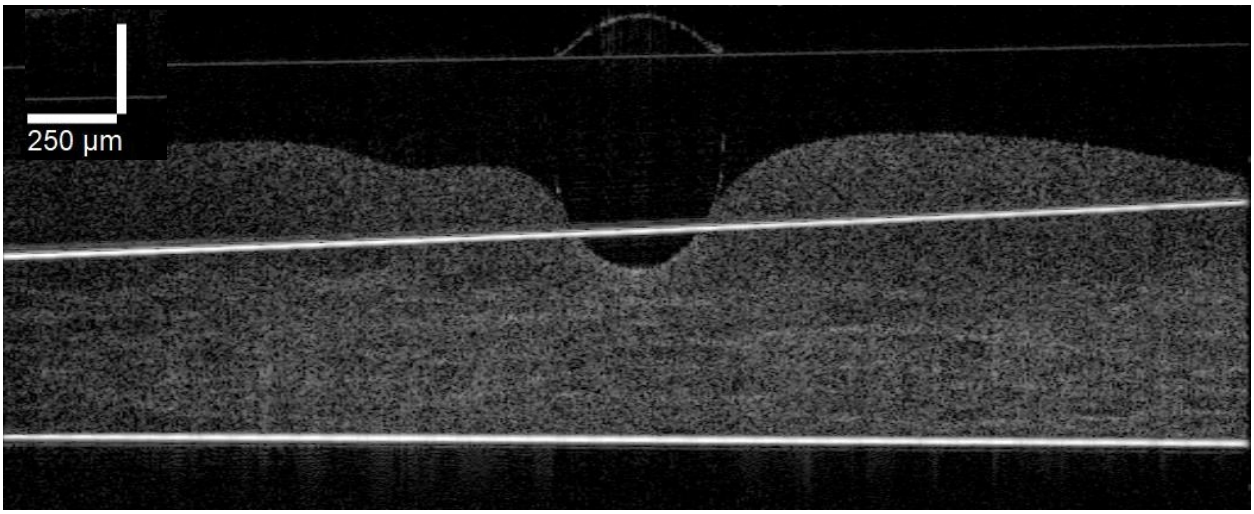

Figure 2.5: OCT scan of bead indentation

2.5 Method Validation

For calibration and method validation, we performed indentations on a standard soft gel substrate of known low stiffness. A thin layer of Cytosoft gel (≈0.5 mm thick) was prepared in a six-well plate as a reference with a nominal Young's modulus of 2 kP [9]. We tested this gel using four different steel bead diameters: 0.5 mm, 0.8 mm, 1.0 mm, and 1.5 mm. Prior to testing, we determined the mass of each steel bead by measuring their density. This was done by weighing a collection of beads on a precise scale and dividing by the count, yielding an average density for each size. The 1.5 mm steel beads were found to have an average density of ~8.25 g/cm³, while the 0.5 mm beads appeared denser (~9.61 g/cm³), likely due to measurement uncertainty at such small mass scales. These densities (close to the expected ~7.8 g/cm³ for steel) were used to calculate each bead's weight (force = mass × 9.81 m/s²).

Figure 2.6: 0.8mm Density vs Number of Beads

Figure 2.7: 1mm Density vs Number of Beads

Figure 2.8: 1.5mm Density vs Number of Beads

In each test, a steel bead was gently placed on the gel's surface (with the gel sample submerged in PBS to keep it hydrated and to negate surface tension effects [10]). The bead, under the influence of gravity, indented the soft gel until equilibrium (its own weight provided a constant force F on the gel). The OCT imaging (figure 1) captured the cross-section of the bead pressing into the gel, from which we measured the indentation depth δ. This procedure is analogous to other reported micro-indentation methods where a known spherical weight is used to indent a gel

and the deformation is measured optically [11]. We repeated this test for all four bead sizes on the same type of soft gel and obtained force indentation data for each. In theory, if the Hertz model holds, all indenter sizes should yield the same effective modulus for the gel. Using the measured F (from the bead's weight) and δ (from OCT), we applied the Hertz contact equation for a sphere on an elastic half-space to compute the gel's apparent Young's modulus [4]. This served as a check that our experimental setup and analysis could correctly recover the gel's known stiffness across different indenter geometries.

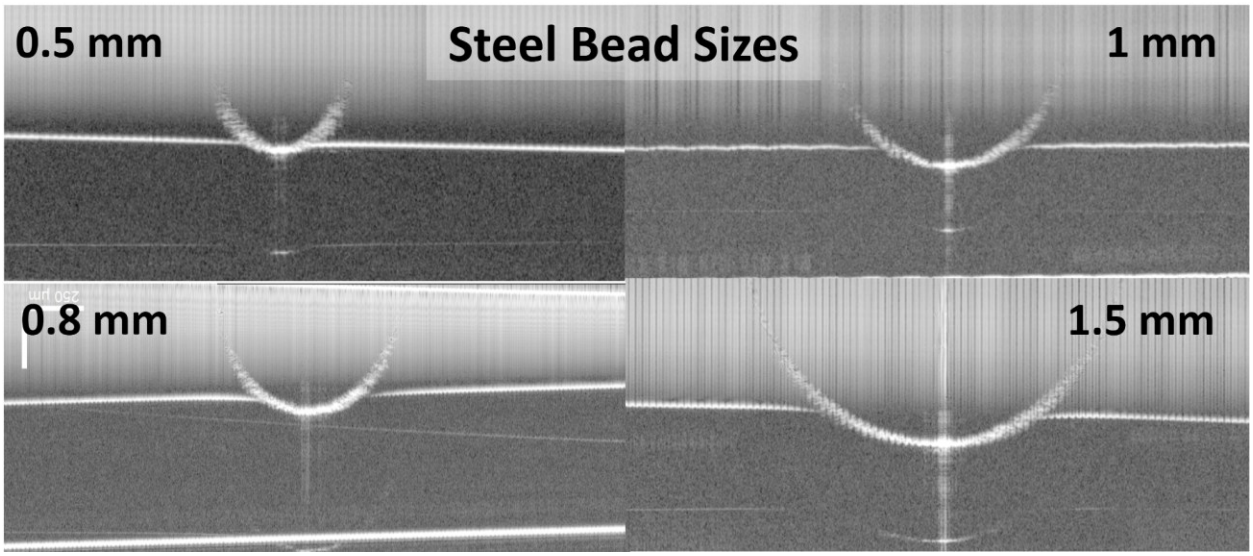

Figure 2.9: Steel bead indentations

2.5.1 Finite-thickness correction of spherical indentation measurements

The Hertz contact theory is based on a semi-infinite half-space assumption. However, this model is not strictly satisfied in this method validation. The CytoSoft reference substrate is a 0.5 mm thin gel on a rigid plastic support. Long et al. used finite element simulations of spherical indentation on soft surfaces to create a model that corrects instances where the gel thickness is close to the indenter radius and indentation depth [11]. They showed that a dimensionless factor ψ can be multiplied by the Hertz modulus to create a corrected modulus. They reported this correction in the regime $0.5 \leq \frac{R}{h} \leq 12.7$ and $\frac{\delta}{h} \leq \min(0.6, \frac{R}{h})$, with R the bead radius, h the gel thickness, and δ the indentation depth [10].

For this experiment, the frictionless ("slip") version of the Long et al. model was used [11]. This maintains consistency with the assumption of frictionless bead-gel contact and with indentation performed in PBS. The correction factor was calculated as

$$\Psi = E/E_H$$

with

$$\Psi = \frac{1 + 2.3\omega}{1 + 1.15\omega^{1/3} + \alpha(R/h)\omega + \beta(R/h)\omega^2}$$

and

$$\omega = (\frac{R\delta}{h^2})^{3/2}$$

For the slip condition,

$$\alpha(\frac{R}{h}) = 10.05 - 0.63\sqrt{\frac{h}{R}}(3.1 + \frac{h^2}{R^2})$$

And

$$\beta(\frac{R}{h}) = 4.8 - 4.23\frac{h^2}{R^2}$$

These expressions are the fitted analytical form reported by Long et al. [11].

The Hertz modulus E_H was first calculated from the standard spherical Hertz equation mentioned above after attaining the measured bead force and OCT indentation depth. The finite-thickness correction factor ψ was then computed for each bead size using the measured R, δ, and the reference-gel thickness h=0.5 mm. This procedure was applied to the CytoSoft calibration dataset to overcome the thin layer progressive stiffening effects.

2.6 Finite Element Modeling of Microindentation

We developed a 2D axisymmetric finite element model in ANSYS Mechanical to simulate the bead indentation experiment. Instead of modeling the full 3D sphere and gel, we drew a cross-sectional slice: a half circle indenter ("bead") in contact with a rectangular gel layer. By enforcing axisymmetric boundary conditions, this 2D slice is mathematically revolved about the vertical axis, effectively recreating a full 3D spherical indentation into a circular gel domain [12]. The gel domain was made much larger in radius than the indenter to emulate an infinite half-space, and the bottom boundary of the gel was fixed (no displacement) [12]. A frictionless contact was defined between the bead and gel surfaces. This symmetry-reduced model significantly lowers computational effort while still capturing the correct contact mechanics, and its accuracy for elastic contact will be verified by comparing results against the classical Hertz theory [12].

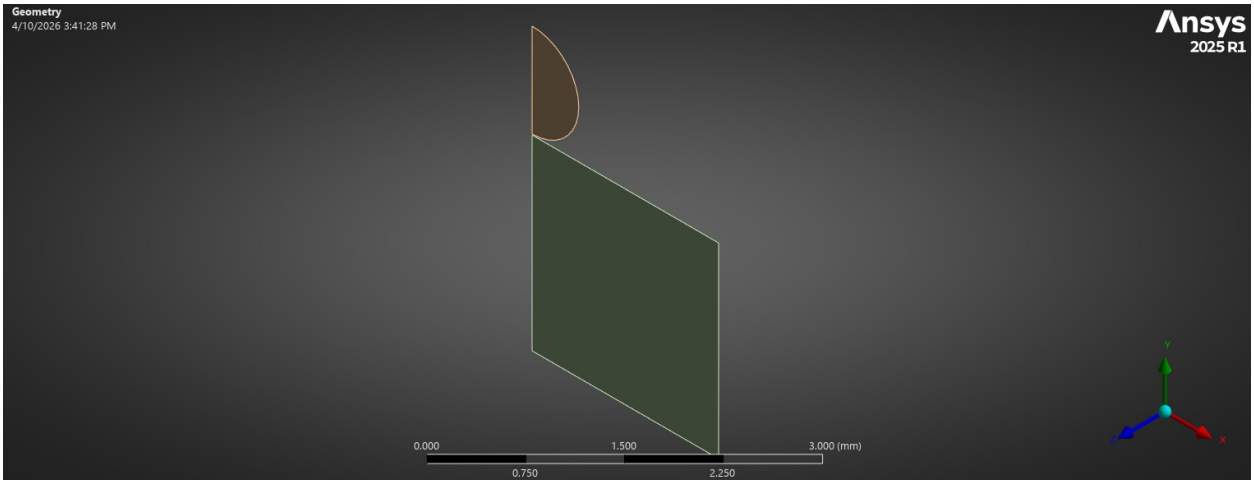

Figure 2.10: Ansys Model

For material properties, the gel was defined as a very soft, linear elastic material with a Young's modulus of 10,000 Pa and a near-incompressible Poisson's ratio ($\nu \approx 0.40$, to represent a hydrated hydrogel). The indenter was assigned the program's properties of structural steel, making it effectively rigid relative to the gel's compliance. This large stiffness mismatch ensures that almost all deformation occurs in the gel, consistent with the experimental scenario. The simulation was set up with a refined mesh in the contact region under the bead to accurately capture the deformation profile [12]. We imposed a prescribed vertical displacement on the bead

(downward into the gel) to an indentation depth of 0.2 mm, and the solver computed the reaction force on the indenter caused by the gel's resistance. By performing a series of indentations (varying the displacement δ), we obtain a force–displacement data from the model. This numerically generated F–δ pair is the simulated version of the physical bead-on-gel experiment, showing how a gel of known stiffness responds to a spherical indenter at a given depth.

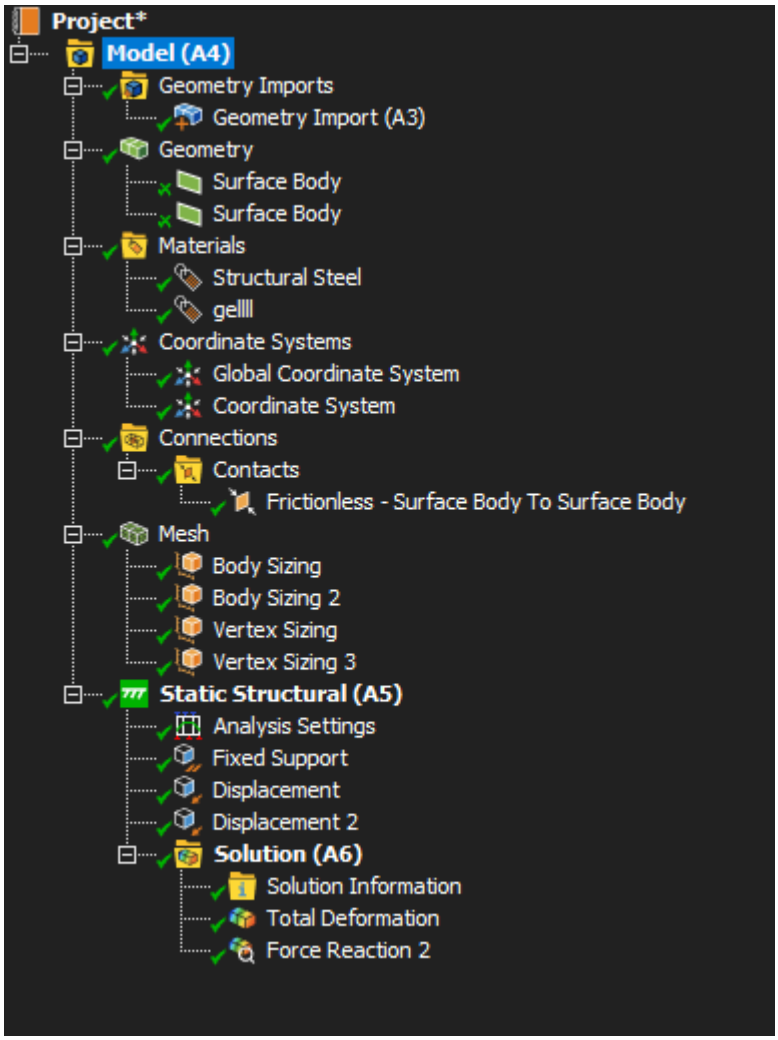

Figure 2.11: Ansys Mechanical Tree Layout

The indenter was displaced downward in 100 incremental load steps. At each step, the bead displacement and corresponding reaction force from the force probe were tracked. Those results were then transported to an excel file. The Hertz contact theory equation was then applied within Excel to calculate the elastic modulus, E, at each of the 100 steps. Finally, the calculated

modulus values were plotted against indentation depth. This provided a visual how the estimated stiffness varied throughout the indentation process.

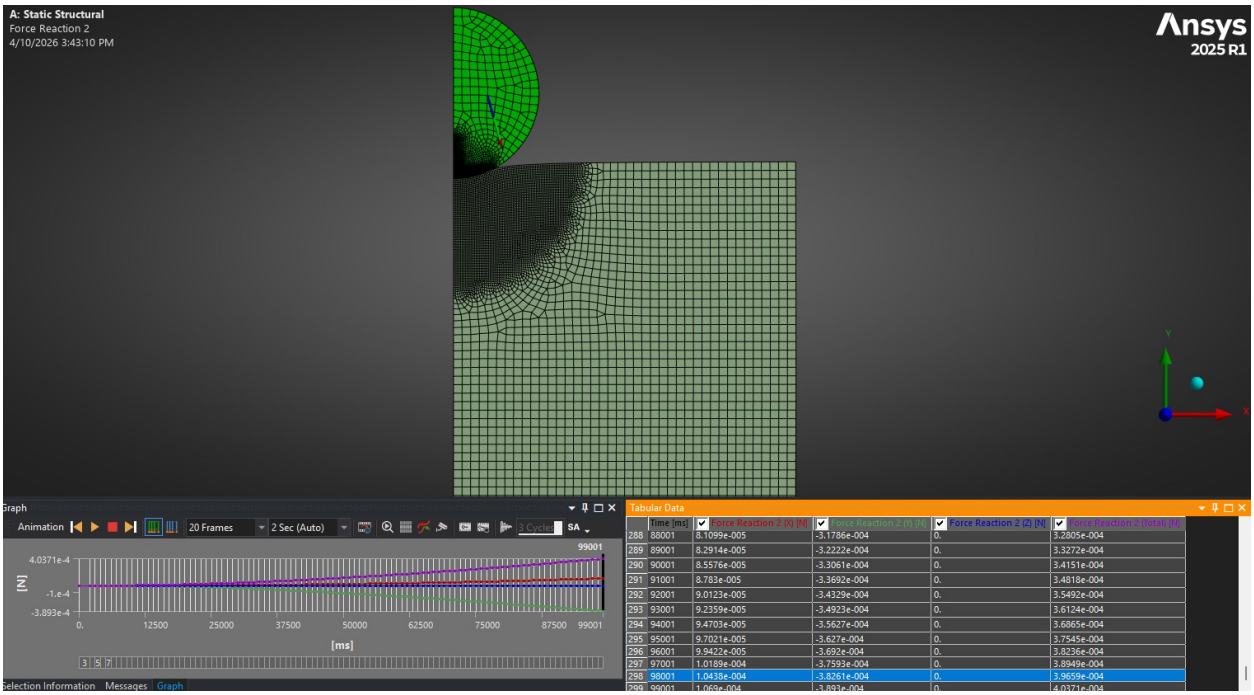

Figure 2.12: Ansys Displacement Visualization

3 Results

3.1 Compaction of FPCM During Development

Six fibroblast-populated collagen matrices ("lattices") were tracked over seven days using OCT bead indentation. Four lattices were controls (Lattices 1, 3, 5, 6) and two lattices were cultured with glyoxal in the medium (Lattices 2, 4). For all FPCM tests, a 0.5 mm diameter glass bead was used as the indenter. Each day, OCT images were used to measure matrix height and indentation depth. Two OCT scans were recorded per lattice (scan 1 and scan 2), and the daily value was taken as the average of the two scans. The indentation load was treated as constant gravity-driven. For the 0.5 mm glass bead, the measured forces used in the spreadsheet were: Weight = 1.605 μN, buoyant force = 0.642 μN, and net indentation force = 0.963 μN. Using the measured indentation depth δ and bead radius R, an apparent Young's modulus E was calculated from the Hertz spherical indentation relationship (as described in the Methods section).

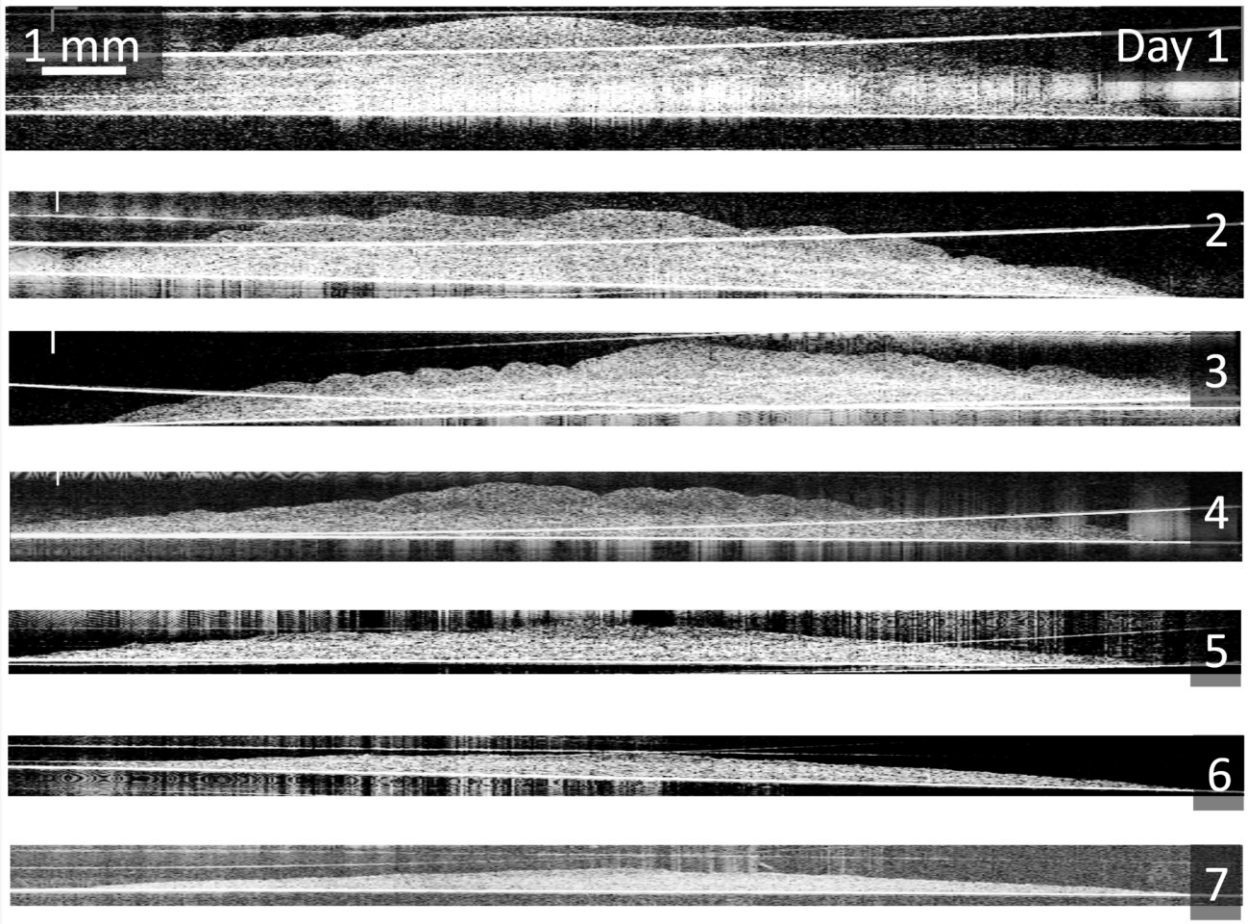

Figure 3.1: FPCM compaction scans over time

A clear finding is that the controls contracted strongly, while glyoxal samples remained taller. Matrix height decreased over time for all lattices, but the magnitude and rate of decrease were very different between groups (Figure PR-2). Control lattices showed rapid compaction from Day 1 to Day 7, with heights dropping from approximately ~1.05-1.14 mm (Day 1) down to ~0.23-0.34 mm (Day 7). Using group averages, the control height decreased from about 1.10 mm (Day 1) to about 0.29 mm (Day 7), which is a reduction of around 75%.

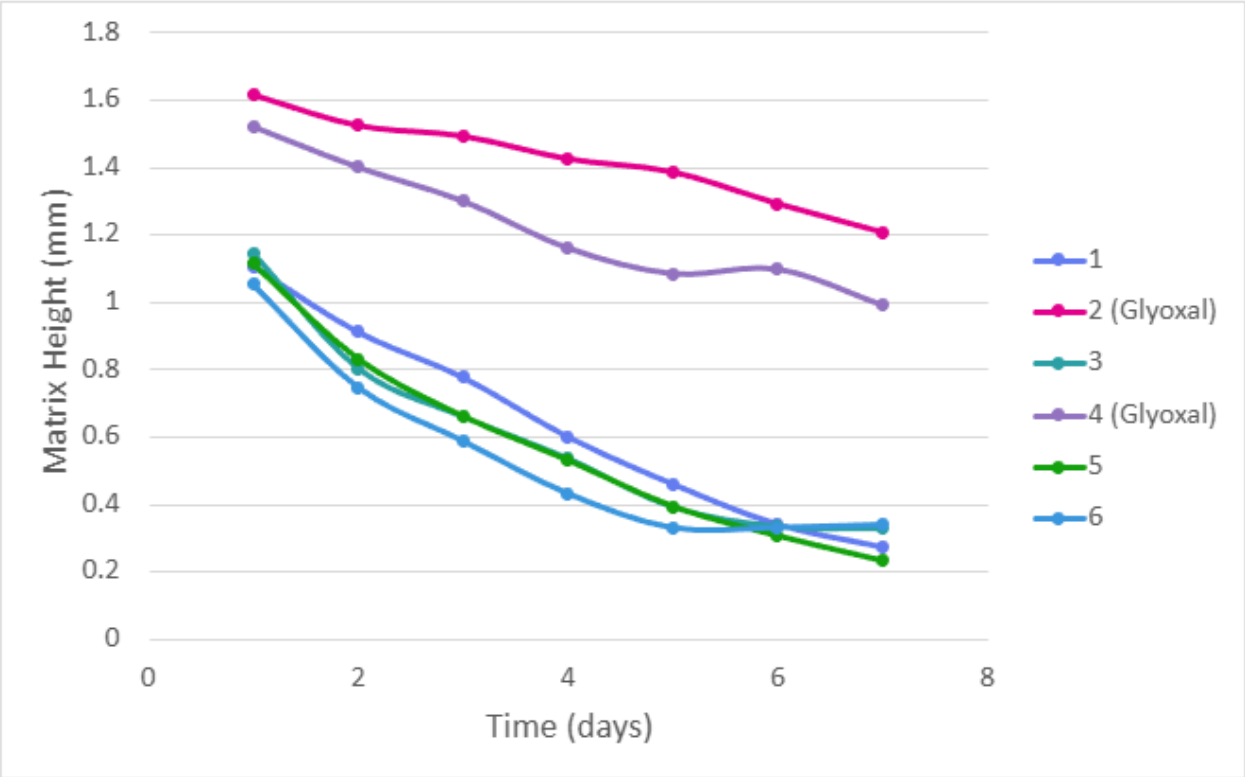

Figure 3.2: Matrix Height vs Time.

Glyoxal lattices remained much taller throughout the experiment. Heights started around ~1.52-1.61 mm (Day 1) and stayed near ~0.99-1.21 mm (Day 7). On average, glyoxal height decreased from about 1.57 mm (Day 1) to about 1.10 mm (Day 7), a reduction of roughly 30%. This sustained thickness in glyoxal samples gives a qualitative observation that glyoxal matrices stay bigger and less contracted than controls.

3.2 Remodeling of FPCM During Development

Indentation depth generally decreased over time for the control lattices (Figure PR-3). Early in the experiment, control indentation depths were typically in the range of ~0.35-0.43 mm (Day 1). Later on, control indentation depths were much smaller, typically ~0.05-0.11 mm by Day 7 Lattice number six results were skewed on the last two days due to human error; there was an unacceptable loss of culture medium. Control indentation decreased from about 0.387 mm (Day 1) to about 0.077 mm (Day 7) showing a 80% reduction.

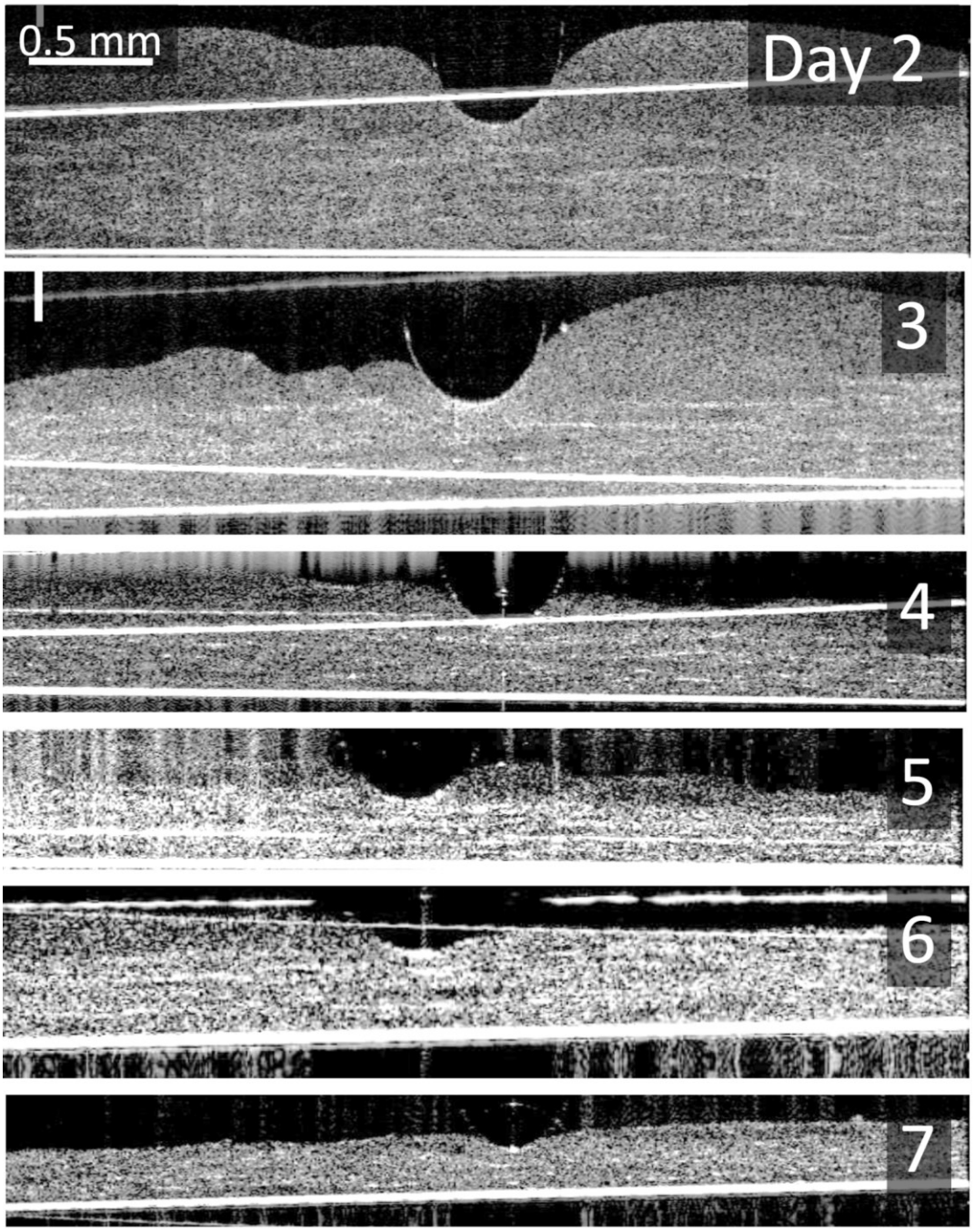

Figure 3.3: Indentation scans over time.

Glyoxal lattices showed smaller changes in indentation depth over time. Indentation depths were around ~0.22-0.31 mm (Day 1) and remained around ~0.15–0.18 mm (Day 7). On average, glyoxal indentation decreased from about 0.264 mm (Day 1) to about 0.164 mm (Day 7) which is a 38% reduction.

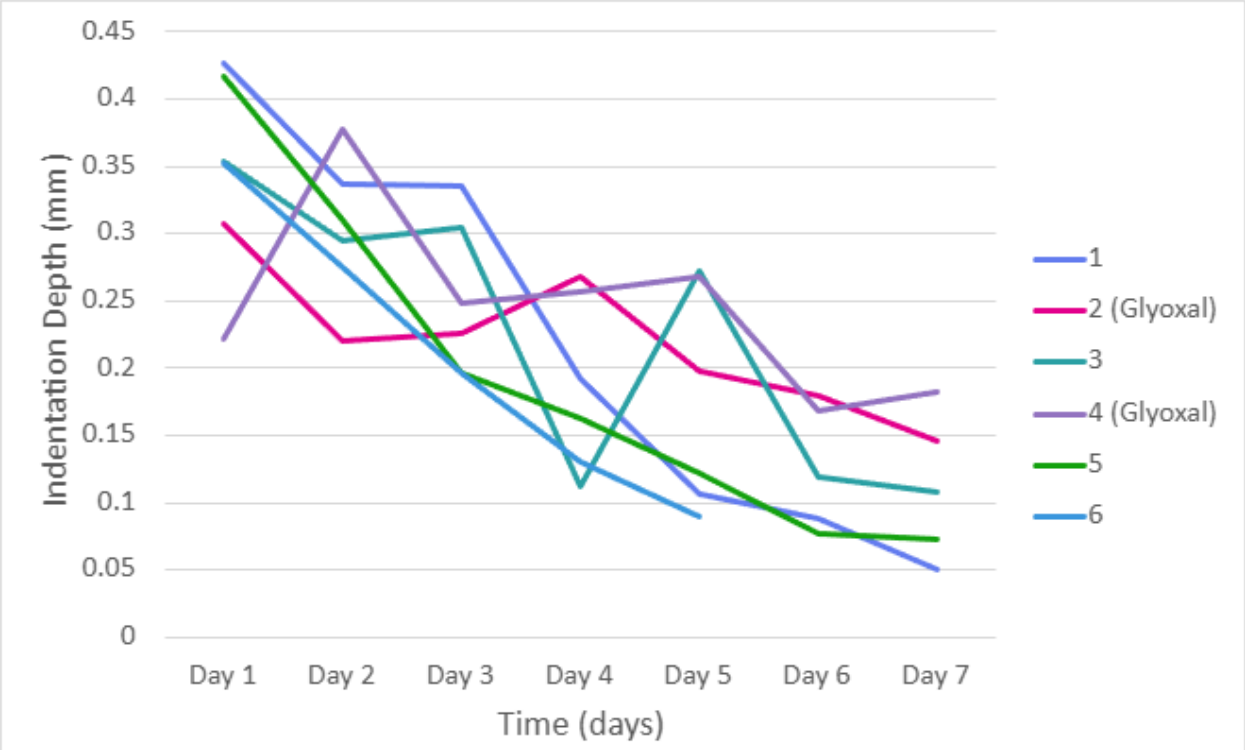

Figure 3.4: Indentation depth vs time.

Apparent modulus increased strongly in controls but remained low in glyoxal samples The control matrices showed a steady increase in apparent modulus across the week. Mean ± SD values for controls were:

Day	Control E (Pa)	Glyoxal E (Pa)
1	4.56 ± 0.71	8.36 ± 2.81
2	6.52 ± 0.83	7.60 ± 4.13
3	9.20 ± 3.71	9.44 ± 0.95
4	20.25 ± 7.07	8.06 ± 0.35
5	26.09 ± 13.72	10.08 ± 3.21
6	32.26 ± 17.86	14.99 ± 1.04
7	60.25 ± 32.08	16.67 ± 3.92

Table 3.1: Calculated modulus of elasticity of FPCM over 7 days.

Overall, the control group increased by about thirteen times from Day 1 to Day 7 going from 4.56 to 60.25 Pa. The standard deviation also increased over time, indicating growing sample to sample variability as remodeling progressed. Contrastingly, the glyoxal-treated matrices stayed in a lower stiffness range after the early time intervals. From Day 4 onward, the controls became substantially stiffer than the glyoxal group, and by Day 7 the control mean modulus was roughly 3-4 times higher than glyoxal.

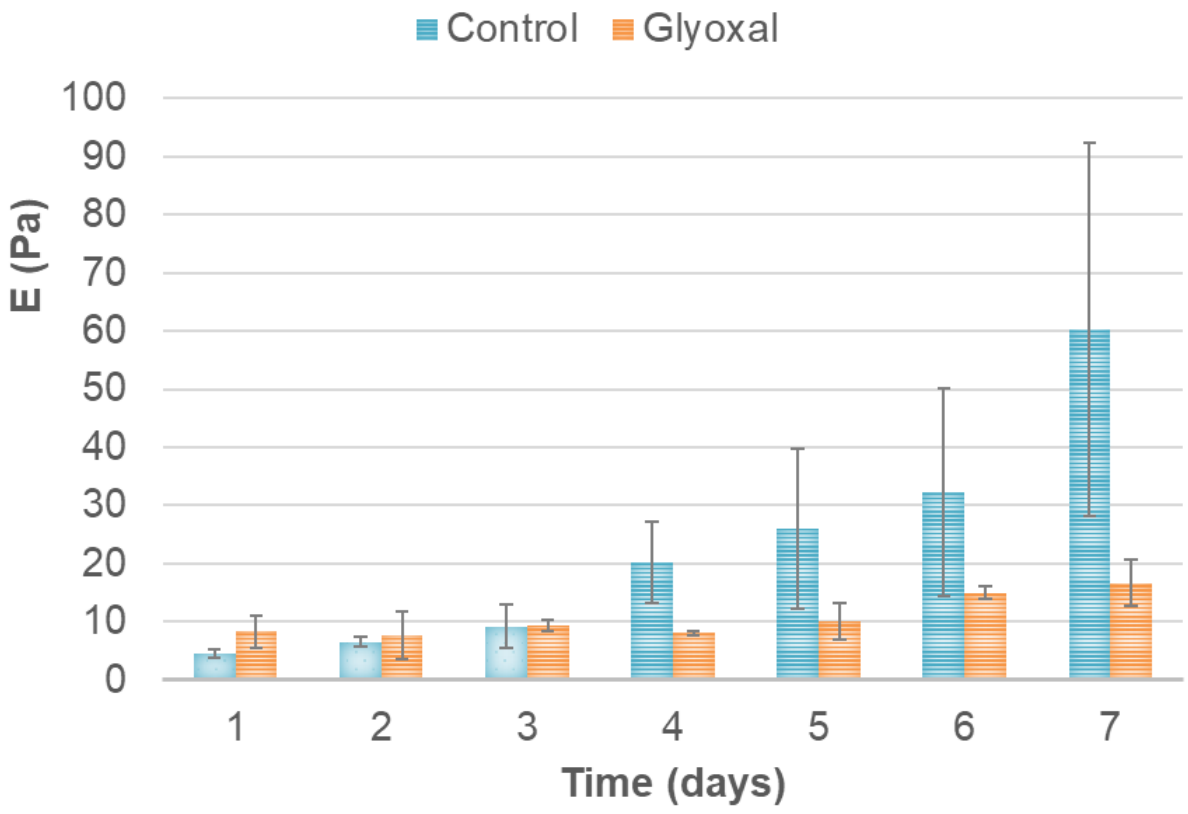

Figure 3.5: E vs Time.

Across the dataset, the trends in modulus, matrix height, and indentation depth were consistent. Controls had a large drop in height, a large drop in indentation depth, and a large rise in apparent

modulus. These results reveal strong contraction, smaller deformation under constant bead load, and steady stiffening over time. Glyoxal samples had less contraction, larger indentation depths at later days, and a less steep rise in modulus.

Since the bead load was constant, decreases in indentation depth over time directly correspond to an increased resistance to deformation. When processed through the Hertz model, this produces the observed increase in apparent modulus. The control group shows the strongest decrease in indentation depth and the largest increase in modulus. Such findings support the conclusion that the control matrices underwent substantial remodeling and stiffening over the seven day period, while glyoxal treatment slowed the stiffening.

3.3 Verification of Microindentation with Reference Gels

To validate the bead indentation assay on a material with a known stiffness, we tested a CytoSoft reference gel labeled 2 kPa and 8kPa using four steel bead diameters (0.5, 0.8, 1.0, and 1.5 mm) [9]. For each bead, we measured the indentation depth and computed an apparent Young's modulus using the Hertz spherical indentation equation just like before. This test also checks whether the computed modulus is consistent across bead sizes. Ideally it would be if all Hertz assumptions were perfectly met and the gel behaved like a semi-infinite linear elastic solid.

The Indentation depth on the nominal 2 kPa and 8 kPa gels increased as bead size increased (Figure R-4 - R-5). This is an expected trend because larger beads are heavier and therefore produce larger deformations. Using density based bead masses, the indentation forces used for modulus were calculated. The apparent Young's modulus values were calculated using the Hertz spherical indentation equation with each bead's F,δ, and R. The value remained below the stated nominal and depended on bead size.

2 kPa Cytosoft gel			
Steel bead diameter (mm)	**Indent force (µN)**	**Indentation depth (mm)**	**Calculated E (Pa)**
0.5	5.52	0.062	398.43 ± 39.89
0.8	18.46	0.091	607.90 ± 78.56
1.0	36.06	0.121	680.00 ± 18.77
1.5	125.89	0.163	1241.30 ± 43.52

Table 3.1: 2 kPa Cytosoft gel indentation results

8 kPa Cytosoft gel			
Steel bead diameter (mm)	**Indent force (µN)**	**Indentation depth (mm)**	**Calculated E (Pa)**
1.0	36.06	0.056	2142.23 ± 155.52
1.5	125.89	0.073	4160.23 ± 70.03

Table 3.2: 8 kPa Cytosoft gel indentation results

Figure 3.6: Indentation vs Steel Bead Size

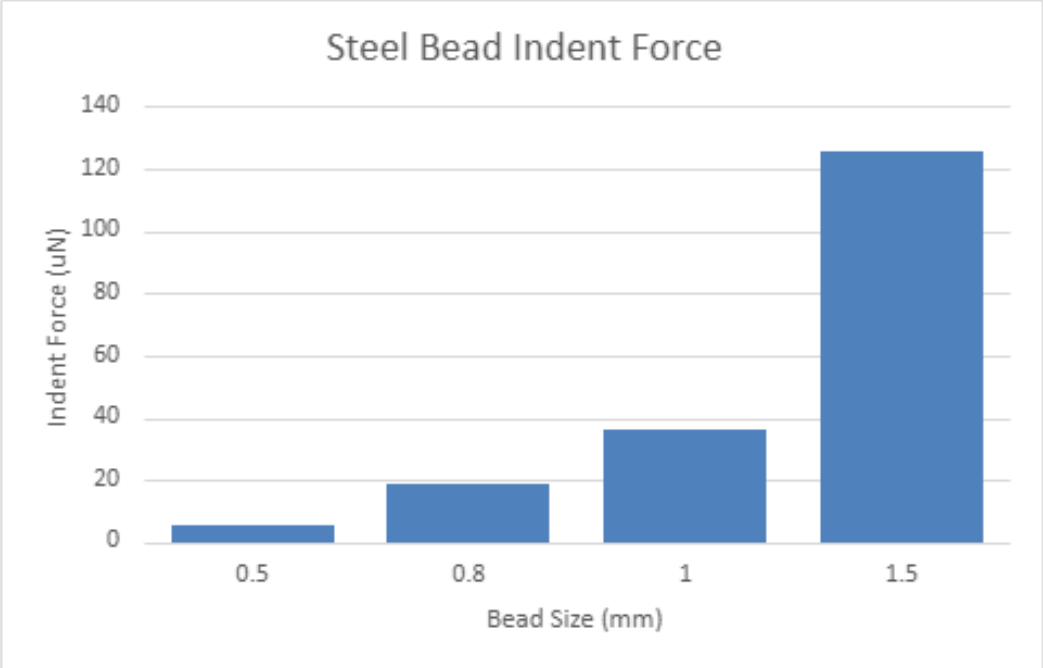

Figure 3.7: Indent Force vs Bead Size.

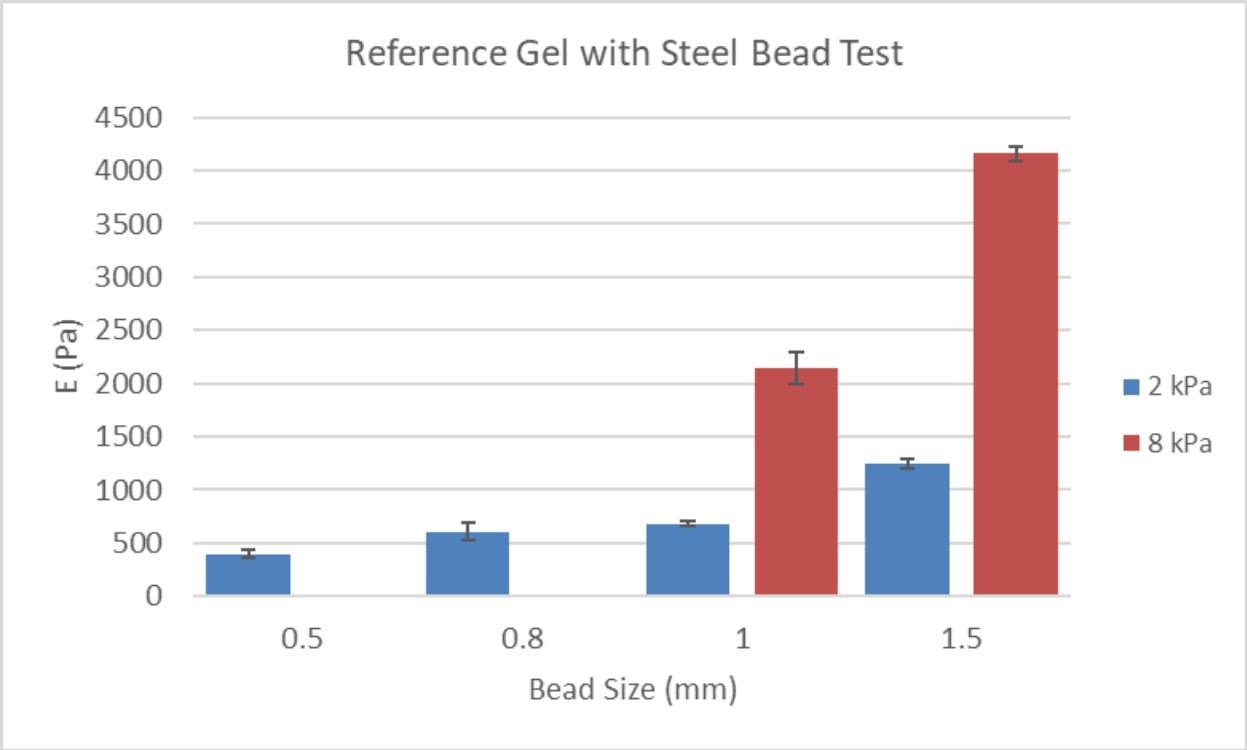

Figure 3.8: Modulus of Elasticity vs Bead Size for 2 kPa and 8 kPa reference gels.

The results ranged from 0.40 kPa to 1.24 kPa, which is approximately 20%-62% of the nominal 2 kPa. Ideally, if the Hertz assumptions were met and the test geometry behaved like a semi-infinite elastic half-space, E should be bead-size independent. Instead, the 1.5 mm bead produced an E about 3.1 times higher than the 0.5 mm bead. An average across bead sizes gives an overall apparent modulus of approximately 0.73 kPa, which is far below the nominal 2 kPa [9]. However, the bead/size dependence is an objective result of this experiment, not an error. The result reveals that the test is not operating in a perfectly ideal Hertz regime for this substrate and configuration.

3.3.1 Finite-Thickness Corrected Modulus for Reference Gels

A finite-thickness correction was applied to the silicone-gel indentation results. This is meant to correct the fact that these tests were performed on thin gel layers supported by a rigid plastic substrate rather than on a semi-infinite elastic half-space. In the original Hertz analysis of the nominal 2 kPa CytoSoft gel, the calculated modulus increased with bead size. It ranged from

398.4 Pa for the 0.5 mm bead to 1241.3 Pa for the 1.5 mm bead, giving an average of approximately 0.73 kPa. The CytoSoft layer was approximately 0.5 mm thick and the thin layer violates Hertz assumptions.

After applying the finite-thickness correction, the corrected moduli for the nominal 2 kPa gel became 307.3, 379.3, 351.5, and 446.9 Pa for the 0.5, 0.8, 1.0, and 1.5 mm steel beads, respectively. The corrected average modulus was 371.3 Pa. And so, the correction did not move the measurements closer to the nominal 2 kPa value. However, it did reduce the spread between bead sizes. Before correction, the largest bead gave a modulus about 3.1 times larger than the smallest bead. After correction, that ratio decreased to about 1.46. The finite-thickness correction improved internal consistency across bead sizes.

The same correction was then applied to a 8 kPa Cytosoft silicone gel dataset tested with 1.0 and 1.5 mm beads [10]. The uncorrected Hertz moduli for that dataset were 2142.2 and 4160.2 Pa. After finite-thickness correction, the values became 1394.6 and 2133.3 Pa, giving an average corrected modulus of 1764.0 Pa. As with the 2 kPa gel, the correction reduced the difference between bead sizes. The ratio between the larger bead and smaller bead modulus decreased from about 1.94 before correction to about 1.53 after correction. However, the corrected values stayed well below the nominal 8 kPa stiffness.

These results show that finite-thickness effects were relevant in the thin silicone-gel configuration. It reduced bead-to-bead variation. Even so, the correction alone did not reconcile the indentation-derived modulus with the manufacturer's values. This is important because the manufacturer modulus was obtained using a fundamentally different measurement technique [10]. Centrifugal loading of embedded beads gives a much different value than localized static surface indentation.

2 kPa Gel					
Bead size (mm)	**Hertz E_H (Pa)**	**Force (μN)**	**Indentation δ (mm)**	**Correction factor Ψ**	**Finite-thickness corrected (E) (Pa)**
0.5	398.43 ± 39.89	5.52	0.063	0.771	**307.37**
0.8	607.90 ± 78.56	18.46	0.091	0.624	**379.35**
1.0	680.00 ± 18.77	36.06	0.121	0.517	**351.52**
1.5	1241.30 ± 43.52	125.89	0.163	0.360	**446.97**

Table 3.3: Finite-thickness corrected modulus for 2 kpa gel

8 kPa Gel					
Bead size (mm)	**Hertz E_H (Pa)**	**Force (μN)**	**Indentation δ (mm)**	**Correction factor Ψ**	**Finite-thickness corrected (E) (Pa)**
1.0	2142.23 ± 155.52	36.06	0.056	0.651	**1394.64**
1.5	4160.23 ± 70.03	125.89	0.073	0.513	**2133.32**

Table 3.4: Finite-thickness corrected modulus for 8 kpa gel

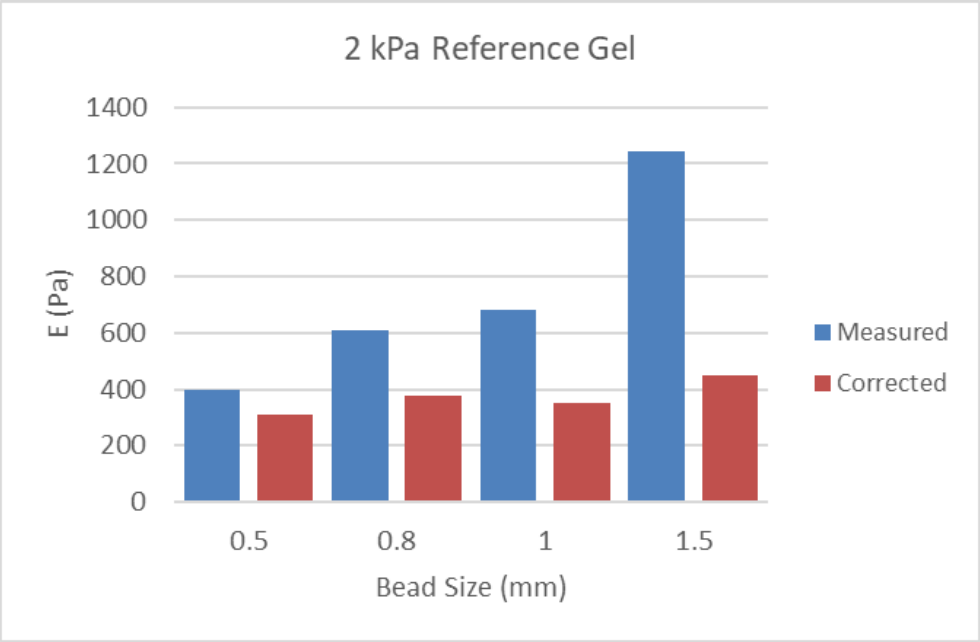

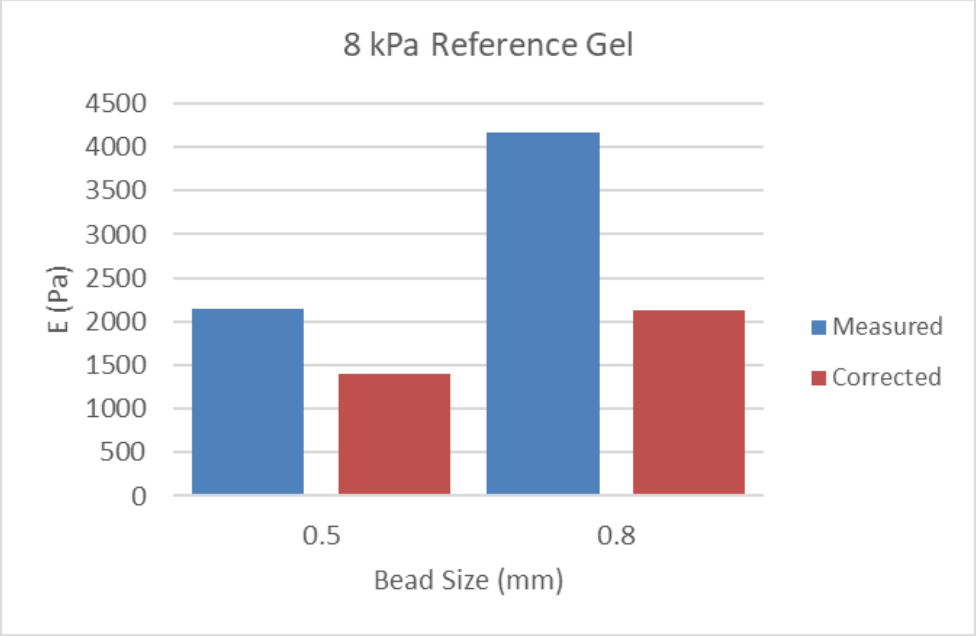

When the average finite-thickness-corrected modulus values were compared with the nominal manufacturer values, both silicone reference gels showed a similar proportional offset. The nominal 2 kPa gel had an average corrected modulus of 371.25 Pa. This means the measured value was 0.186 times the nominal value, or conversely, the nominal value was 5.39 times larger than the measured value. The nominal 8 kPa gel had an average corrected modulus of 1763.98

Pa. This means the measured value was 0.220 times the nominal value, or conversely, the nominal value was 4.54 times larger than the measured value.

Nominal E (Pa)	Average Corrected E (Pa)	Corrected E / Nominal E	Nominal E / Corrected E
2000	371.25	0.186	5.39
8000	1763.98	0.220	4.54

Table 3.5: Corrected E ratio from nominal value

These similar ratios indicate that the OCT bead indentation method produces a relatively consistent proportional offset across gels of different nominal stiffness. The corrected modulus values were not equal to the manufacturer values, but they were lower by a comparable ratio. The nominal-to-measured ratio was 5.39 for the 2 kPa gel and 4.54 for the 8 kPa gel, meaning the 8 kPa gel showed a slightly smaller offset but remained in the same general proportional range. Because the manufacturer values were obtained using a fundamentally different method based on centrifugal loading of embedded beads rather than localized static surface indentation, exact agreement was not expected. Instead, this result suggests that the present method captures stiffness in a repeatable and systematic way.

3.4 Finite Element Analysis Results

The ANSYS Mechanical bead indentation model was successfully solved and then refined by a mesh sensitivity study. After getting to a converged solution, progressively finer meshes were tested to determine how mesh density influenced the calculated modulus of elasticity. The gel material in the model was assigned a Young's modulus of 10,000 Pa. Results showed that finer meshes produced higher calculated modulus values and reached the assigned material modulus at smaller indentation depths.

For example, with a mesh size of 0.05 mm, the calculated modulus reached the assigned value of 10,000 Pa at an indentation depth of about 0.026 mm. When the mesh was refined to 0.005 mm, the same modulus value was reached at an indentation depth of approximately 0.014 mm. Based on this study, the final mesh selected for the model was 0.005 mm on the bead and 0.01 mm on the gel. This provided an optimal balance between numerical accuracy and computational efficiency.

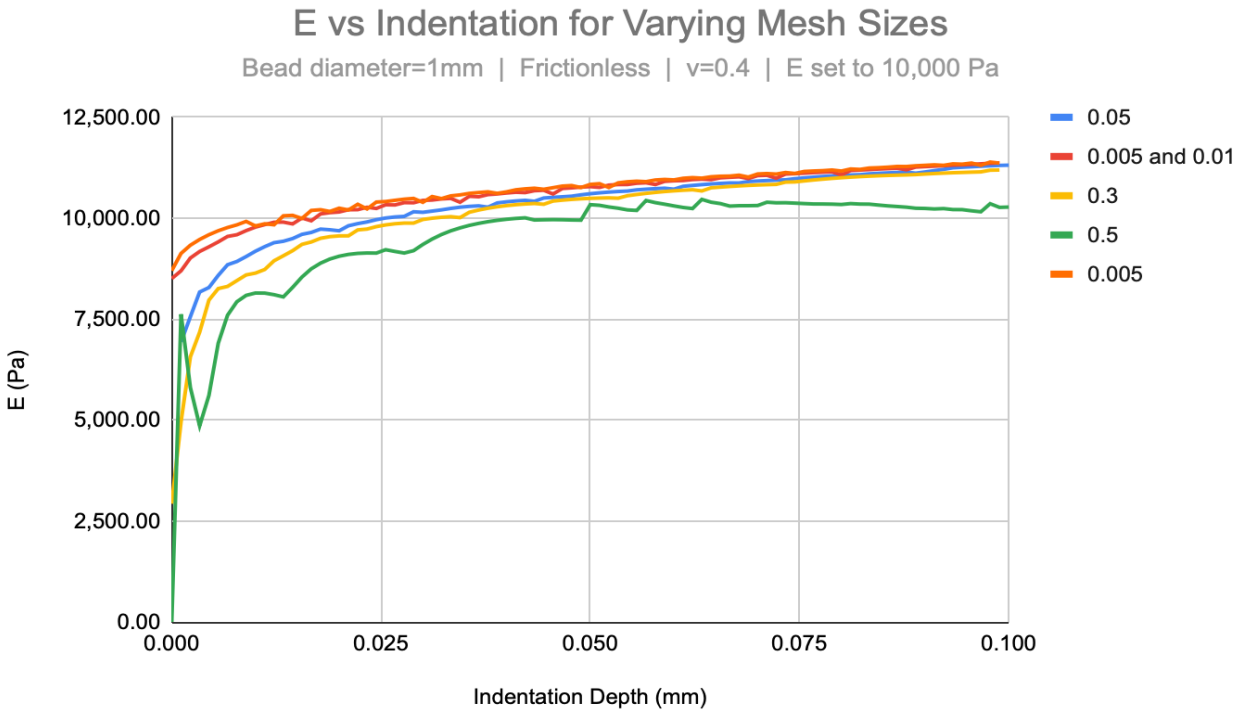

Figure 3.9: E vs Indentation for Varying Mesh Sizes (mm)

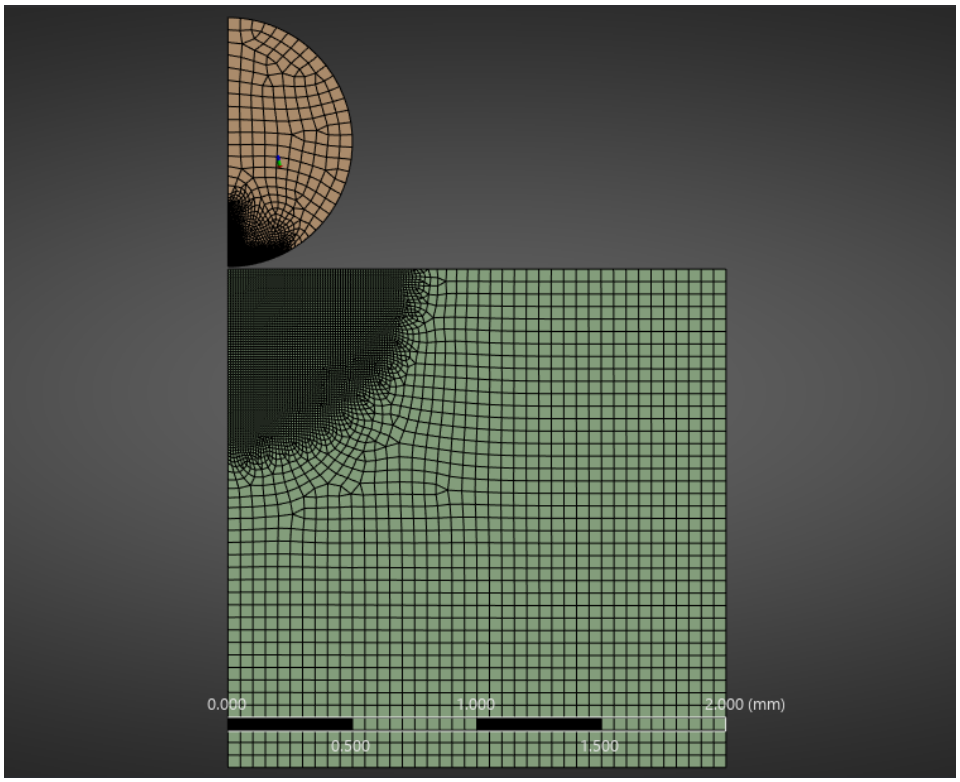

Figure 3.10: 0.005 mm ball and 0.01 mm gel were the optimal mesh sizes

The final results show that the Hertz-calculated modulus converges toward the prescribed material modulus at very small indentation depths. At the initial stage of contact, the calculated modulus appears low. This is because of numerical contact initialization and insufficient resolution right at the point of bead-gel contact. As the mesh becomes finer, the model reaches the assigned modulus more quickly, which indicates that mesh refinement improves the accuracy of the contact solution near the beginning of indentation.

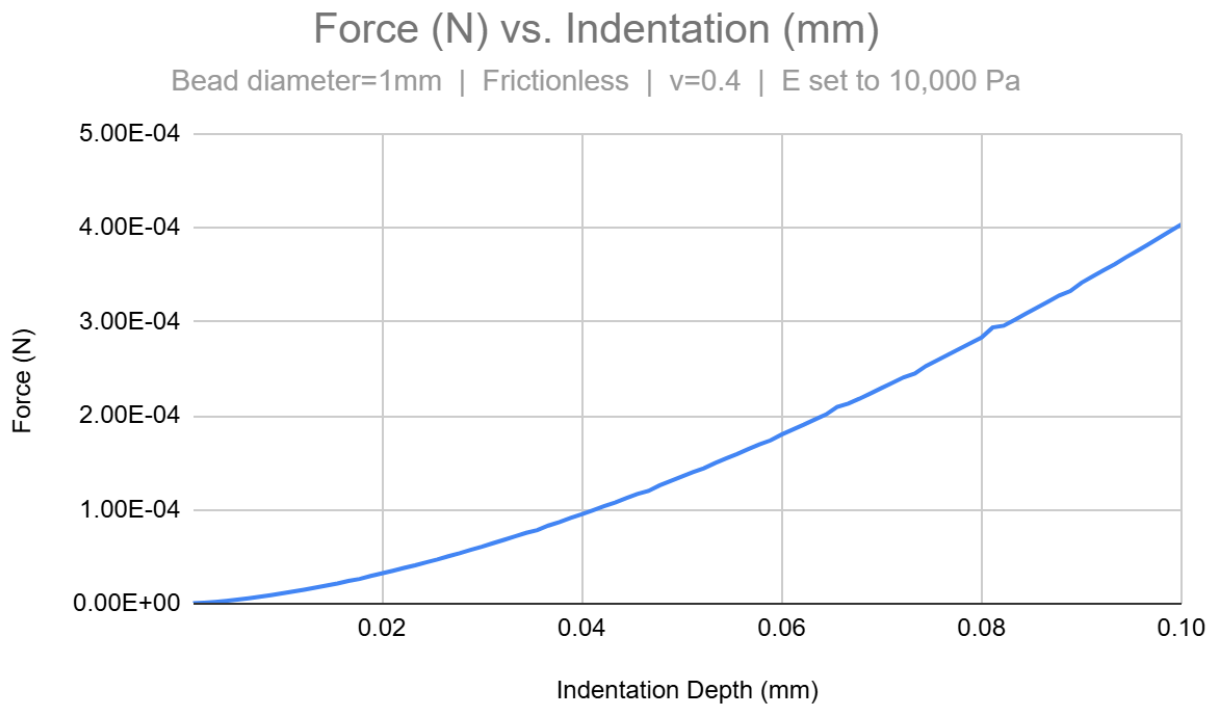

Figure 3.11: Ansys model force vs Indentation

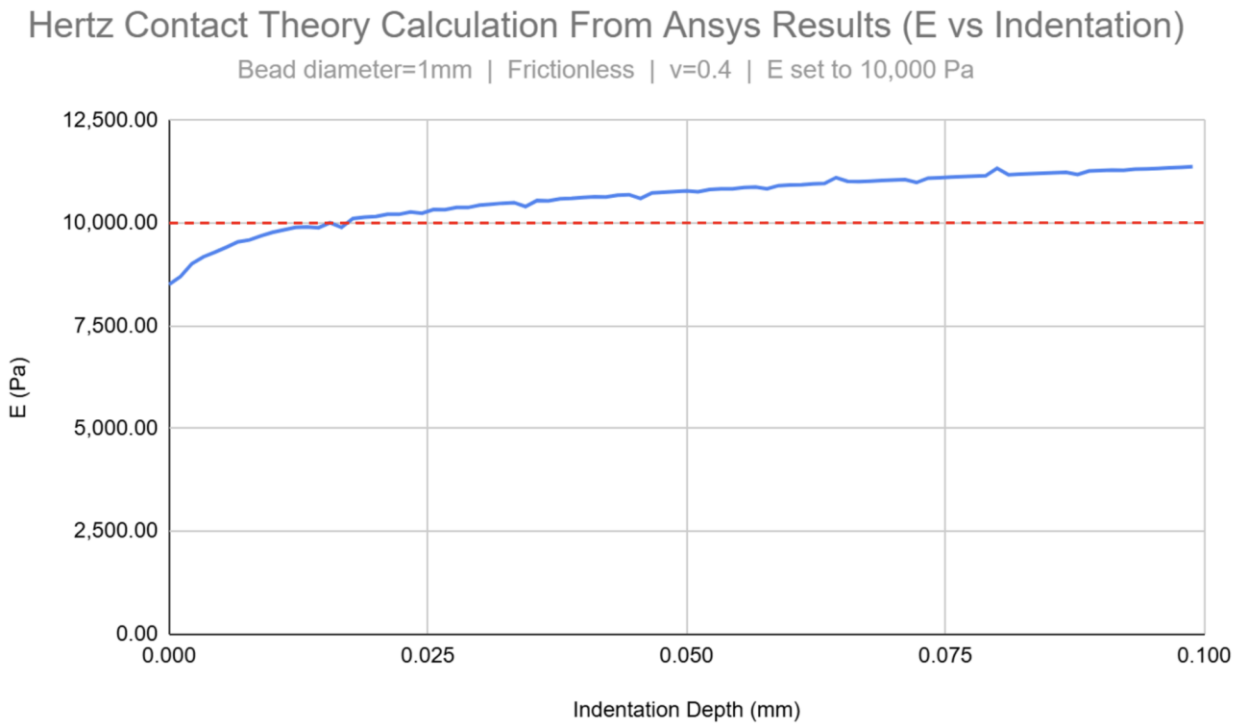

Figure 3.12: Hertz Contact Theory Calculation From Ansys Results

Taking the average from the whole indentation range (0 - 0.1mm), the calculated modulus remained slightly above the assigned value. Because the ANSYS model was defined as linear elastic, this effect should not be interpreted as viscoelasticity [12]. Instead, it is more likely caused by numerical effects associated with mesh density and the increasing number of elements resisting deformation as indentation progresses [13]. Overall, these results indicate that the Hertz contact solution agrees best with the finite element model at small indentation depths. Larger indentations show increasing deviation from the set value of E.

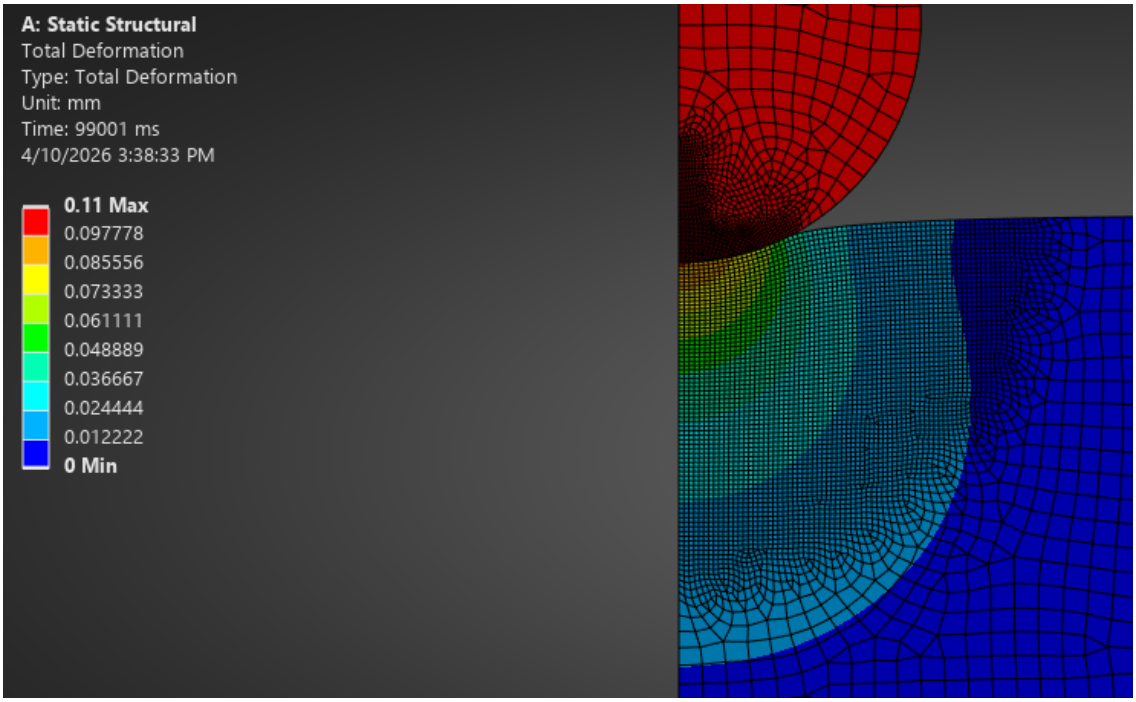

Figure 3.13: Deformation at gel-bead contact

3.4.1 Effect of Friction Coefficient

A second simulation study was performed to quantify the effect of contact friction on the calculated modulus of elasticity. Three friction coefficients were tested: 0.2, 0.5, and 0.8. For each case, the average modulus of elasticity was calculated over an indentation depth range of 0.1 mm. The frictionless case had an average calculated modulus of 10,611.66 Pa.

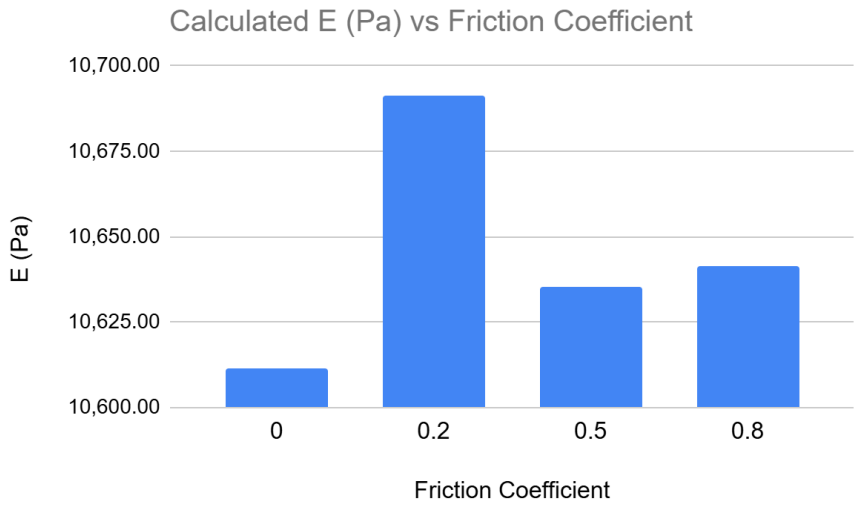

Figure 3.14: Calculated E (Pa) vs Friction Coefficient

Adding friction didn't make much of a difference. For a friction coefficient of 0.2, the average calculated modulus was 10,691.28 Pa. For a friction coefficient of 0.5, the average modulus was 10,635.15 Pa. For a friction coefficient of 0.8, the average modulus was 10,641.30 Pa. These differences were small relative to the overall modulus value, indicating that friction had minimal influence on the calculated modulus in this model. Therefore, within the tested range, contact friction was not a major factor affecting the Hertz-based stiffness calculation.

4 Discussion

4.1 Monitoring FPCM Remodeling

The strongest result of this study is that it captured remodeling in fibroblast populated collagen matrices in a clear, repeatable, biologically meaningful way. In the control lattices, apparent modulus increased significantly across the week while matrix height and indentation depth fell in parallel. The glyoxal treated matrices remained taller, indented more deeply, and stiffened much less. That pattern is exactly what would be expected if active fibroblast remodeling compacted and tensioned the collagen network in controls, while glyoxal altered or slowed that remodeling response. Having a larger sample size would have helped to reduce the standard deviation across the data. Prior work on fibroblasts in 3D collagen, anchored collagen compaction measured by OCT, and collagen-gel contraction assays likewise shows that compaction and mechanical change are tightly coupled metrics [1, 3, 7]. The present data therefore support the central conclusion that the method is highly effective for relative day-to-day tracking of FPCM remodeling.

A key advantage of this method is that it combines a simple and repeatable gravity based loading condition with a direct high resolution measurement of defamation. The OCT cross-section images allow the indentation depth to be measured directly and precisely. This non-invasive approach allows the same FPCM to be measured again and again over a multiple day span without mechanically damaging anything. Such qualities are perfect for monitoring the dynamics of cell remodeling. When the same bead, same force, and same imaging geometry are used repeatedly, changes from one day to the next are highly interpretable. Prior OCT-based micro-indentation work with OCT captured deformation under a spherical indenter at constant force in soft hydrogels/tissues help to affirm the effectiveness of this system [4]. One key thing to note is that the modulus obtained should be treated as an apparent local modulus rather than a universal bulk material constant because it depends on ideal sphere contact, elastic half-space behavior, and on how the contact point and indentation depth are defined [13].

4.2 The Biologically Meaningful Modulus

A simple way to explain viscoelasticity is that a soft hydrated matrix behaves partly like a spring and partly like a fluid-filled dashpot. If it is loaded quickly, it resists more strongly and appears stiffer; if it is loaded slowly or held under load, the network and fluid have time to rearrange, so the same material can deform more and appear softer. That time dependence shows up as creep under constant load and as stress relaxation under constant deformation. It also shows up directly in indentation experiments. In hydrogel microindentation, measured Young's modulus increases with indentation speed, while slower quasi-static measurements reduce the contribution of time-dependent effects. In other words, there is not just one modulus unless the material is truly purely elastic; there is an early, faster response and a later, more relaxed response [18].

This matters a lot in this study because the material is not just a regular foam or rubber. It is a living collagen matrix that cells are actively pulling on, moving through, and remodeling over time. Cells do this slowly, over seconds to hours. Because of that, cells probably do not mainly experience the very fast, instant stiffness of the matrix. If the matrix has time to relax while the cells are pulling on it, then the cells are really interacting with a softer, more relaxed resistance. For that reason, the slowest and most relaxed stiffness measurement in this study is likely the most biologically meaningful one [19].

This also explains why faster tests can give higher stiffness values without being more "correct." A fast indentation can make the matrix look stiffer because the material has not had time to relax yet. A slower or held indentation can make it look softer because creep and stress relaxation have had time to happen. For a cell-remodeled collagen matrix, the slower, quasi-static value is probably more relevant for understanding what the cells are actually sensing, while the faster value may be more useful for comparison with standard material tests [19].

A related issue is poroelasticity. In a hydrated matrix, time dependence does not have to come only from viscoelasticity. It can also come from fluid flow through the porous network. Poroelasticity means that when the bead pushes into the matrix, the solid skeleton deforms, pore pressure rises, and fluid redistributes with time. That makes the response depend on loading rate, hold time, and contact size. Spherical indentation is actually one of the standard ways poroelastic effects are studied in soft tissues. That means part of the apparent softening during slow or held

measurements could be true viscoelastic relaxation, part could be poroelastic fluid redistribution, and part could be both at once. Recognizing that distinction strengthens the discussion, because it turns a limitation into a testable hypothesis for future work [17].

4.3 Calibration on Nominal Stiffness Gels

The CytoSoft calibration experiments are best interpreted as showing a systematic difference in measurement method compared to manufacturer values. The present study revealed the assay is not yet absolutely calibrated for thin, supported silicone layers under these exact conditions. However, the results were not random. The method produced a repeatable trend and a consistent offset. In other words, the assay appears to capture stiffness in a stable and systematic way, even if the absolute values do not yet match the vendor certified numbers exactly [14].

A major reason for this offset is that the current method measures stiffness in a different way from the manufacturer. Advanced BioMatrix report that CytoSoft stiffness is certified by tracking how marker particles move relative to one another across the bonded silicone layer during centrifugation [10]. Placing a rigid spherical bead on top of the surface and measuring local indentation with OCT is different. The vendor's method is a bonded layer calibration of the silicone substrate under a different loading geometry. The OCT method is a local, normal-contact indentation interpreted with Hertz theory. Those two approaches do not apply the same type of stress, do not use the same contact area, do not sample the same volume of material, and do not impose the same boundary conditions [15]. It is therefore unsurprising that they produce different absolute numbers, even when they rank stiffness in the same general order.

Hertz contact theory assumes a semi-infinite elastic half-space, but the CytoSoft substrate used here was a thin silicone layer, approximately 0.5 mm thick, bonded to a rigid plastic support. Under those conditions, the rigid base can affect the stress field and make the Hertz-derived modulus bead-dependent [16].

This is why the finite-thickness correction is an important technical finding in this research. After applying the correction, the absolute values still did not rise into the manufacturer's range, but the bead-to-bead spread became much smaller. For the nominal 2 kPa gel, the ratio between the largest-bead and smallest-bead modulus dropped from about 3.1 before correction to about

1.46 after correction. For the nominal 8 kPa gel, that ratio dropped from about 1.94 to about 1.53. This means the correction removed a real source of artifact related to supported-layer geometry and improved the internal consistency of the assay across indenter sizes [11].

An especially important result is that the average finite-thickness corrected modulus values showed a very similar percent difference from the manufacturer values for both silicone reference gels. The nominal 2 kPa gel had an average corrected modulus of 371.25 Pa, corresponding to a percent difference of 137.37%, while the nominal 8 kPa gel had an average corrected modulus of 1763.98 Pa, corresponding to a percent difference of 127.74%. Those similar percent differences suggest that the OCT bead-indentation method produces a relatively consistent proportional offset across gels of different nominal stiffness. That is important because it indicates the method is not failing randomly. Instead, it is responding in a repeatable and systematic way across different stiffness levels. This supports the idea that the discrepancy is modelable and potentially calibratable in future work.

Taken together, the steel bead CytoSoft results show that the OCT assay is useful, but its output must be interpreted carefully. For thin supported silicone layers, the present method should not yet be treated as an absolute replacement for the manufacturer calibration. However, it clearly captures stiffness related changes in a systematic and repeatable way. Furthermore, the finite-thickness correction moves the method in the right direction by reducing bead-size dependence.

4.4 Simulation Defined the Valid Hertz Regime

In the simulation, the gel was defined as linear elastic, nearly incompressible, and axisymmetric. Under those conditions, the Hertz-calculated modulus converged toward the prescribed value once the very earliest contact-establishment stage had passed. That is exactly the outcome that should be expected [13]. The simulation therefore supports the claim that the force and indentation data are being interpreted appropriately within the small-indentation regime. This is consistent with the broader indentation literature showing that Hertz theory is acceptable for soft synthetic gels at small deformation, but becomes progressively less reliable as indentation strain

and geometric nonlinearity increase [20]. This simulation is a validation of the intended use window of the Hertz model, not a claim that Hertz remains exact for every indentation depth.

The very small effect of friction in the ANSYS study also has a reasonable mechanical explanation. The loading here is almost entirely normal compression, not sliding. For soft materials that are close to incompressible, the radial displacement at the contact is limited enough that assuming frictionless contact is often acceptable in normal indentation [21]. Friction usually matters more when lateral constraint is strong, when the layer is thin and bonded, or when tangential motion is important [21].

4.5 Advantages, Limitations, and Best-Use Cases

This method has several advantages. The applied load is simple to calculate from bead weight and buoyancy, so there is no need for complicated calibration hardware. OCT provides a direct cross-sectional image of the event being mechanically analyzed, giving load geometry and the measured displacement [4]. The test is gentle enough to repeat on living matrices, spatially local enough to resolve regional behavior, and simple enough to use as a day-by-day assay during FPCM development. Those are not small benefits. In mechanobiology, methods that are easy to repeat, easy to interpret visually, and compatible with wet living samples often end up being more useful than methods that are theoretically purer but experimentally difficult.

In terms of limitations, the reported modulus depends on indenter radius, sample thickness, indentation depth, hydration state, contact-point definition, and the assumption that Hertz theory is appropriate. In hydrated matrices, viscoelasticity and poroelasticity can both shift the apparent modulus. In supported thin layers, finite-thickness and substrate effects can be large. In heterogeneous matrices, different test locations can legitimately produce different values. For all of those reasons, the method at its current stage is best described as measuring a local apparent modulus under a defined protocol, not a universal material constant that should match every independent reference method [14].

Those strengths and limitations point to the best application of the method. It is especially well suited for monitoring treatment effects, remodeling trajectories, and relative stiffness changes in

soft living matrices over time. It is less well suited, at least in its present form, for claiming exact agreement with certified bulk or bonded-layer modulus values obtained by very different loading methods. In wound-healing, fibrosis, and tissue-engineering contexts, however, the relative question is often the biologically important one: did the matrix stiffen, soften, compact, or respond differently to a treatment? For that class of question, the OCT bead-indentation assay is highly useful [4].

4.6 Conclusion and Future Work

The clearest takeaways from this work are straightforward. First, OCT bead indentation is a strong method for relative tracking of FPCM remodeling, because it clearly resolves day-to-day changes in indentation depth, thickness, and apparent modulus under the same simple loading condition [1]. Second, the most biologically meaningful number for a cell remodeled collagen matrix is the slower, more relaxed, quasi-static modulus, because cells interact with viscoelastic matrices over finite time and do not only probe the instantaneous response [18]. Third, the finite-thickness correction made the assay more internally consistent by reducing bead-to-bead variation on supported silicone gels [11]. Fourth, the combined steel-bead and simulation results suggest that the present method captures stiffness in a repeatable systematic way, but with a method-specific offset that still requires calibration when absolute values are the goal [13].

The most useful future work follows directly from those points. Real time OCT imaging during bead placement and during the hold period would allow the force–displacement history to be separated into an early response and a relaxed response, making it possible to quantify creep or stress relaxation directly. A time dependent load-tracking study would test how much of the measured response is viscoelastic. A wet versus partially dry comparison could help determine whether pore-fluid redistribution contributes appreciably to the indentation response and therefore whether poroelasticity is important [17]. Finally, applying the assay at multiple regions on the same lattice would convert it from a single-point tracker into a true spatial map of remodeling. Those steps would preserve the method's simplicity while making the reported modulus more interpretable across materials and experiments.

Overall, this study shows that OCT-based spherical bead indentation is a valuable tool for following how living collagen matrices change over time. Its present form is best understood as a minimally invasive, spatially resolved, static assay of local matrix mechanics rather than a universal replacement for every other modulus test. Framed that way, the method is not limited by the fact that different test geometries give different absolute values. It is useful because it can monitor the mechanical environment that cells are actually remodeling, day by day, in the same wet culture setting where the biology is happening.

References

[1] M. B. Vaughan, G. Xu, T. L. Morris, P. Kshetri, and J. X. Herwig, “Predictable fibroblast tension generation by measuring compaction of anchored collagen matrices using microscopy and optical coherence tomography,” *Cell Adhesion & Migration*, vol. 13, no. 1, pp. 303–314, 2019, doi: 10.1080/19336918.2019.1644855.

[2] J. Kanta, “Collagen matrix as a tool in studying fibroblastic cell behavior,” *Cell Adhesion & Migration*, vol. 9, no. 4, pp. 308–316, 2015.

[3] S. Rhee, “Fibroblasts in three dimensional matrices: cell migration and matrix remodeling,” *Experimental & Molecular Medicine*, vol. 41, no. 12, pp. 858–865, 2009.

[4] Y. Yang, P. O. Bagnaninchi, M. Ahearne, R. K. Wang, and K. K. Liu, “A novel optical coherence tomography-based micro-indentation technique for mechanical characterization of hydrogels,” *Journal of the Royal Society Interface*, vol. 4, no. 17, pp. 1169–1173, 2007.

[5] Y.-W. Chen *et al.*, “Integrin αV mediated activation of myofibroblast via mechanoparacrine of transforming growth factor β1 in promoting fibrous scar formation after myocardial infarction,” *Biochemical and Biophysical Research Communications*, vol. 692, Art. 149360, 2024.

[6] M. B. Vaughan, E. W. Howard, and J. J. Tomasek, “Transforming growth factor-beta1 promotes the morphological and functional differentiation of the myofibroblast,” Experimental Cell Research, vol. 257, no. 1, pp. 180–189, 2000, doi: 10.1006/excr.2000.4869.

[7] Q. Zhang, P. Wang, X. Fang, F. Lin, J. Fang, and C. Xiong, “Collagen gel contraction assays: from modelling wound healing to quantifying cellular interactions with three-dimensional extracellular matrices,” *European Journal of Cell Biology*, vol. 101, no. 3, Art. 151253, 2022.

[8] M. Zündel, A. E. Ehret, and E. Mazza, “Factors influencing the determination of cell traction forces,” *PLoS One*, vol. 12, no. 2, Art. e0172927, 2017.

[9] L. Wang and J. P. Stegemann, “Glyoxal crosslinking of cell-seeded chitosan/collagen hydrogels for bone regeneration,” *Acta Biomaterialia*, vol. 7, no. 6, pp. 2410–2417, 2011.

[10] Advanced BioMatrix, “CytoSoft®: Culturing cells on an in vivo softness,” technical note, Mar. 27, 2020.

[11] R. Long, M. S. Hall, M. Wu, and C. Y. Hui, “Effects of gel thickness on microscopic indentation measurements of gel modulus,” *Biophysical Journal*, vol. 101, no. 3, pp. 643–650, 2011.

[12] W. Yan and C. L. Pun, “Spherical indentation of metallic foams,” *Materials Science and Engineering: A*, vol. 527, no. 13–14, pp. 3166–3175, 2010.

[13] J. W. Harding and I. N. Sneddon, “The elastic stresses produced by the indentation of the plane surface of a semi-infinite elastic solid by a rigid punch,” *Mathematical Proceedings of the Cambridge Philosophical Society*, vol. 41, no. 1, pp. 16–26, 1945.

[14] Advanced BioMatrix, “Certificate of Analysis: CytoSoft® Discovery Kit (Catalog #5190, Lot #A154),” Oct. 21, 2024.

[15] Fisher Scientific, “CytoSoft® T-25 flasks, 0.2 kPa,” [Online]. Available: https://www.fishersci.com/shop/products/cytosoft-t-25-flasks-0-2-kpa/502255923 (accessed Dec. 15, 2025).

[16] E. Gutierrez and A. Groisman, “Measurements of elastic moduli of silicone gel substrates with a microfluidic device,” *PLoS One*, vol. 6, no. 9, Art. e25534, 2011.

[17] M. Wang, S. Liu, Z. Xu, K. Qu, M. Li, X. Chen, Q. Xue, G. M. Genin, T. J. Lu, and F. Xu, “Characterizing poroelasticity of biological tissues by spherical indentation: An improved theory for large relaxation,” *Journal of the Mechanics and Physics of Solids*, vol. 138, Art. 103920, 2020, doi: 10.1016/j.jmps.2020.103920.

[18] C. T. Mierke, “Viscoelasticity, Like Forces, Plays a Role in Mechanotransduction,” Frontiers in Cell and Developmental Biology, vol. 10, Art. 789841, 2022, doi: 10.3389/fcell.2022.789841.

[19] Z. Gong, S. E. Szczesny, S. R. Caliari, E. E. Charrier, O. Chaudhuri, X. Cao, Y. Lin, R. L. Mauck, P. A. Janmey, J. A. Burdick, and V. B. Shenoy, “Matching material and cellular timescales maximizes cell spreading on viscoelastic substrates,” Proceedings of the National Academy of Sciences of the United States of America, vol. 115, no. 12, pp. E2686–E2695, 2018, doi: 10.1073/pnas.1716620115.

[20] D. C. Lin, D. I. Shreiber, E. K. Dimitriadis, and F. Horkay, “Spherical indentation of soft matter beyond the Hertzian regime: numerical and experimental validation of hyperelastic models,” Biomechanics and Modeling in Mechanobiology, vol. 8, no. 5, pp. 345–358, 2009, doi: 10.1007/s10237-008-0139-9.

[21] M. J. Wald, J. M. Considine, and K. T. Turner, “Independent measurement of Young’s modulus and Poisson’s ratio of transparent thin films using indentation and surface deformation measurements,” Soft Matter, vol. 22, no. 2, pp. 532–545, 2026, doi: 10.1039/D5SM00804B.

Jackson College of Graduate Studies

Download and fill out the form below. Save it to your device and email it to:
gradcoll@uco.edu

405-974-3417

Thesis Committee Form

Thesis Defense or Project

Student's Name: Joshua Pitzer

UCO Student ID: *20511016 Student's Email: jpitzer@uco.edu

Graduate Program/Major: Engineering / Mechanical Engineering

Graduate Advisor's Name: Dr. Gang Xu

Title of Thesis or Project: CELL-DRIVEN COLLAGEN MATRIX REMODELING MEASURED WITH OCT

Members of Thesis or Project Committee:
(Signatures)

Committee Chairperson Signature

Signature

Signature

Signature

JCGS 4/02/26